1

Li-Ion Battery

Ruiping Liu

China University of Mining & Technology (Beijing), Department of Materials Science and Engineering, 100083, Beijing, China

1.1 Introduction

1.1.1 History of the Lithium-Ion Battery

Lithium is the lightest metal in nature, with an atomic weight of 6.94, a density of $0.534\,g\,cm^{-3}$, and a standard electrode potential of $-3.045\,V$, which is the lowest potential among all the metal electrodes. In the 1970s, the first lithium metal battery was prepared by using titanium sulfide as the cathode and lithium metal as the anode. However, the lithium dendrites caused by the uneven deposition and distribution of lithium during charging will cause a large irreversible loss of active lithium, and even short-circuit of the battery, thus the battery is prohibited from charging [1]. In the 1980s, it is found that the lithium ions can be reversibly and freely embedded into the graphite materials, and soon, the battery was successfully prepared by using graphite as the anode material. Lithium ions can be freely and reversibly inserted and extracted between the cathode and anode, which is visually called "rocking chair battery" and later named "lithium ion battery" [2]. Both of the lithium-ion batteries and lithium metal batteries can work by the insertion and extraction of lithium ions at the electrode. However, compared with the lithium metal battery, the lithium metal can be replaced by other active materials to solve the safety problem of lithium metal as the anode material in lithium-ion battery [3]. As the first company to commercialize lithium-ion batteries, Sony Corporation has done much research work [4, 5]. Currently, commercial lithium-ion batteries mainly use transition metal lithium salts as the positive electrode Li_xM_2 (M represents a transition metal such as Co, Mn, Ni, Fe, etc.), and inexpensive and excellent conductive porous graphite as the negative electrode. They are widely used in digital products, grid energy storage, electric vehicles (EVs), hybrid electric vehicles (HEVs), and etc. [6–9].

1.1.2 Basic Structure of Lithium-Ion Battery

The composition of lithium-ion battery is shown in Figure 1.1. Lithium-ion battery is mainly composed of the following four parts: cathode, anode, electrolyte, and
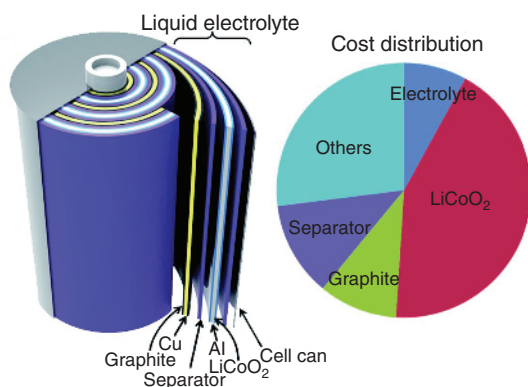
Figure 1.1 Structural illustration and relative cost of each component. Source: Zhou et al. [10]. Reproduced with permission of John Wiley Sons.

separator. The main purpose of cathode materials is to provide lithium ions for the whole battery system. At present, the main positive materials are Li_2M (M = Co, Ni, Mn, and other transition metals) with layered structure, ternary materials (Li [Co, Ni, Mn]$_2$), $LiMn_2O_4$, and $LiMPO_4$ (M = Fe, Co, Ni, Mn, and so on) with spinel structure. The main commercial cathode material of lithium-ion battery is $LiCoO_2$. The cost of the material can account for about half of the total cost of lithium-ion battery. Its theoretical capacity is 274 mAh g^{-1}, and the discharge voltage is 3.6 V [5].

The anode is generally prepared by uniformly loading the active material together with the conductive agent (generally carbon black) and the binder on the current collector, and it is the key part of lithium-ion battery. Currently, the commonly used collector is copper foil with the thickness of 7–15 μm.

The electrolyte in lithium-ion batteries is an important medium for the free transportation of lithium ions between the cathode and anode. The electrolyte is generally composed of lithium salts ($LiPF_6$, $LiClO_4$, and $LiBF_4$) and organic solvents. The common organic solvents are ethylene carbonate (EC), propylene carbonate (PC), dimethyl carbonate (DMC), and diethyl carbonate (DEC).

The function of the separator in the lithium-ion battery is to prevent the anode and cathode from contacting and thus avoiding the short circuit of the battery. The most commonly used membranes are polymer films, including polypropylene (PP) and polyethylene (PE). Generally, the strength of the separator is improved by three-layer structure, and the lithium ions can pass through the separator smoothly.

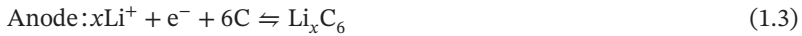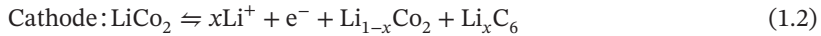### 1.1.3 Working Mechanisms of Lithium-Ion Battery

The working principle of lithium-ion battery is a simply process of lithium-ion continuously embedding and detaching between the cathode and anode. Its essence is a kind of concentration battery. Figure 1.2 shows the working principle of lithium-ion battery [11]. During charging process, the oxidation reaction of the cathode materials is taken place and the lithium ion transfers from the cathode to the anode. The lithium ion is embedded in the anode material after passing through the electrolyte and separator. At the same time, the electron reaches the anode through the external circuit. During the discharge, the lithium ion is removed from the anode and

Figure 1.2 The working principle of lithium-ion battery. Source: Wang et al. [11] Reproduced with permission of Elsevier.
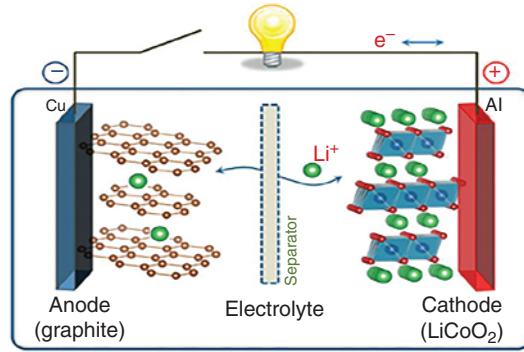
transferred to the cathode and embedded in the cathode materials, accompanied by the electron transfer in the external circuit.

Taking porous graphite as the anode materials, lithium cobaltate ($LiCoO_2$) as the cathode materials, the electrochemical reactions during the charge and discharge process are briefly described as follows:

$$LiCo_2 + 6C \rightleftharpoons Li_{1-x}Co_2 + Li_xC_6 \tag{1.1}$$

$$Cathode: LiCo_2 \rightleftharpoons xLi^+ + e^- + Li_{1-x}Co_2 + Li_xC_6 \tag{1.2}$$

$$Anode: xLi^+ + e^- + 6C \rightleftharpoons Li_xC_6 \tag{1.3}$$

1.1.4 Characteristics of Lithium-Ion Batteries

The advantages of lithium ion batteries are mainly as follows:

- Compared with normal chemical batteries, the lithium-ion battery has a large specific capacity and energy density. The volume of the lithium-ion battery is 20–50% of that of a chemical battery with the same capacity. At this stage, the actual specific energy of the lithium ion battery is 150–200 Wh kg^{-1}, and the specific energy of the lithium ion battery can eventually reach 250–300 Wh kg^{-1}.
- Lithium-ion battery allows a wide working range. Under room temperature, the discharge capacity of the battery accounts for more than 85% of the overall theoretical capacity after one month in an open circuit. Lithium-ion batteries can be discharged steadily in a wide temperature range (−20 to 55 °C).
- Lithium-ion battery can be recycled and used many times. The lithium-ion batteries currently used have avoided the problems of internal lithium dendrite short circuits that cause damage and potential safety hazards. The remaining capacity of the lithium-ion battery with carbon material as the anode is still more than 60% of the theoretical capacity after 1200 cycles, which is much higher than that of other types of batteries.
- Compared with lithium metal battery, lithium-ion battery possesses the resistance characteristics of short circuit, overcharge, overdischarge, and impact. It can be quickly charged and discharged at a current density of 1 C.

- No memory effect exists in lithium-ion battery, and it can be repeatedly charged and discharged.
- Lithium-ion battery can be packed with small size and lightweight.

The shortcomings of lithium-ion batteries are mainly manifested as follows:

- Since the electrolyte of lithium-ion battery mainly consists of organic component, the conductivity is lower than that of a chemical battery on the market, so the corresponding internal circuit impedance is greater than that of a chemical battery.
- The voltage platform of the lithium-ion battery changes greatly (about 40%) during the discharge process, and there is no relatively more stable discharge platform. For a device that requires stable power supply, it is impossible to maximize its efficiency, and also due to the large change in the voltage platform of the lithium-ion battery, it is also difficult to estimate the remaining capacity.
- The cost of battery composition materials is high. The main cost of lithium-ion batteries comes from the relatively expensive cathode material $LiCo_2O_4$.
- A comprehensive battery management system is needed to prevent the lithium-ion battery from overcharging.

1.2 Cathode Materials for Lithium-Ion Batteries

Cathode material is one of the key components of lithium-ion battery, which determines the working voltage, capacity, and cycle life of the battery. At present, the potential cathode materials mainly include layered-structural cathode materials ($LiCoO_2$, $LiMnO_2$, $LiMn_2O_4$, $LiNi_xCo_yMn_zO_2$, and $LiNi_{0.8}Co_{0.15}Al_{0.05}O_2$), spinel structural materials ($LiMn_2O_4$ and $LiNi_{0.5}Mn_{1.5}O_4$), polyanionic materials ($LiFePO_4$, $Li_3V_2(PO_4)_3$, and Li_2FeSiO_4), etc. The ideal cathode material should have the following characteristics: (i) high capacity; (ii) high oxidation reduction potential; (iii) good chemical and thermal stability; (iv) high ionic and electronic conductivity; (v) high safety; (vi) low price.

1.2.1 Layer-Structured Cathode Materials

Common layer-structured cathode materials mainly include lithium cobalt oxide ($LiCoO_2$), lithium nickel oxide ($LiNiO_2$), and lithium manganese oxide ($LiMnO_2$), all of which exhibit the crystal structure of α-$NaFeO_2$. Among them, $LiCoO_2$ with rhombohedral structure is the first commercialized layered cathode material, and the O atom is formed hexagonal dense accumulation according to the order of ABCABC (Figure 1.3). It is first reported by Goodenough in 1981, the theoretical specific capacity of $LiCoO_2$ is 274 mAh g^{-1}, and the average working voltage is 3.9 V (vs. Li/Li$^+$). However, during the actual charging process, the layer structure of Co—O octahedron will become unstable and gradually transition to spinel phase when the amount of lithium removal is more than 50% and thus results in the decrease of battery capacity. Thus, the actual reversible specific capacity of $LiCoO_2$ can only be up to 140 mAh g^{-1}. In addition, the high cost and toxicity of Co limit its application in large-scale energy storage system.
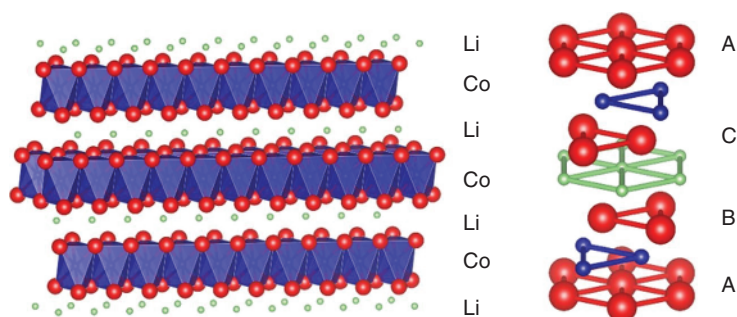
Figure 1.3 Crystal structure diagram of LiCoO$_2$ (red: oxygen, purple: cobalt, green: lithium). Source: Erickson et al [12] Reproduced with permission of IOP Publishing.
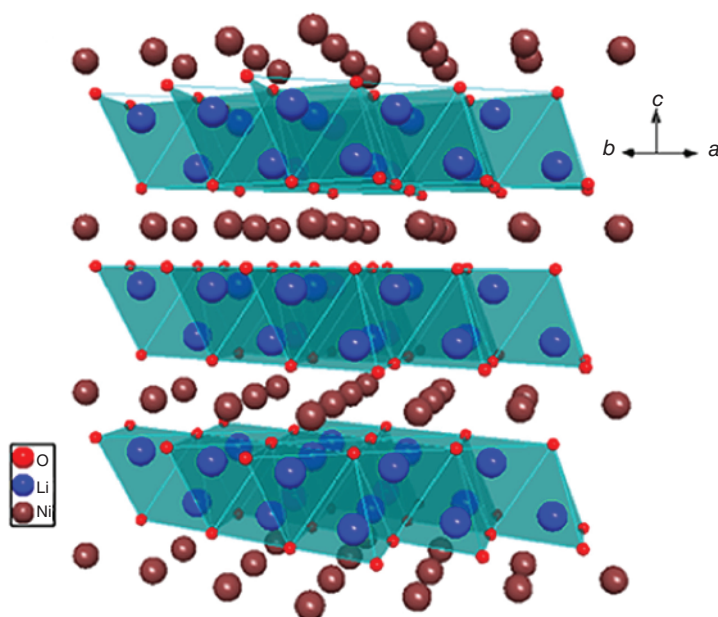

Figure 1.4 Crystal structure diagram of LiNiO$_2$ (red: oxygen, brown: nickel, blue: lithium). Source: Manthiram et al [13]. Reproduced with permission of Elsevier.

As shown in Figure 1.4, the layered LiNiO$_2$ cathode materials have a theoretical specific capacity of 274 mAh g^{-1}, but only 140 mAh g^{-1} can be used in the actual charging and discharging process. During the charging process, lithium ions are removed from the interlayer of LiNiO$_2$, due to the approach of the Ni^{2+} ion radius (0.69) and Li$^+$ (0.76), it is very easy to occupy the lithium position and cause the mixed arrangement of lithium nickel, which will lead to the destruction of the original layered structure, and some lithium ions cannot be re-embedded into LiNiO$_2$ during discharging and thus cause the rapid attenuation of reversible capacity [14]. In addition, it is very difficult to synthesize and unstable at high temperature, the structure will change from hexagonal phase to cubic phase.
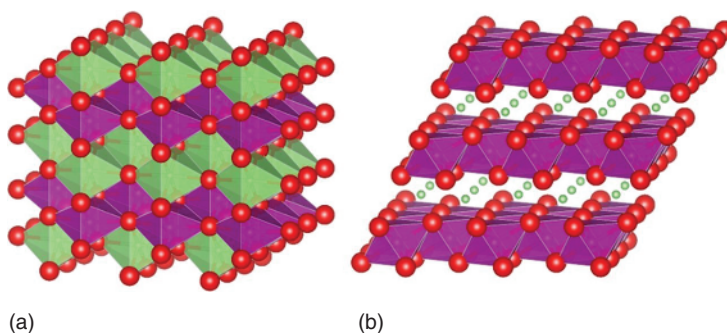
(a)   (b)

Figure 1.5 (a) Orthorhombic LiMnO$_2$ (*Pmmn*), (b) monoclinic LiMnO$_2$ (*C2/m*); (red: oxygen, pink: manganese, green: lithium). Source: Erickson et al [12]. Reproduced with permission of IOP Publishing.

The theoretical specific capacity of LiMnO$_2$ is 285 mAh g^{-1}, and the actual specific capacity is about 165–195 mAh g^{-1}. As shown in Figure 1.5, the layer-structured LiMnO$_2$ belongs to metastable phase, in which Mn^{3+} is prone to disproportionation to form Mn^{2+} and Mn^{4+}. Meanwhile, Mn^{3+} is easy to dissolve and occupy the position of Li$^+$ during the charging process, finally forming Jahn–Teller distortion and causing the damage of layered structure [15]. In addition, it is difficult to synthesize layer-structured LiMnO$_2$ because it is easy to transform into rhombic or spinel structure; thus, the application of pure LiMnO$_2$ as cathode materials is difficult.

As cathode materials of lithium-ion batteries, LiCoO$_2$, LiNiO$_2$, and LiMnO$_2$ exhibit their own shortcomings as cathode, and they cannot be widely used in the field of power batteries. However, it is possible to obtain new cathode materials with high capacity, high voltage, and high cycle stability by preparing Li–Ni–Co–Mn–O ternary materials, in which LiCoO$_2$ has a higher electron and ion transfer rate to ensure the rate performance, the higher capacity of LiNiO$_2$ can provide the cathode a high capacity, and LiMnO$_2$ mainly plays a role in stabilizing the structure. Theoretically, the three components can form any uniform solid solution while maintaining the original layered structure. In the ternary system, Ni, Co, and Mn elements can be randomly distributed in the transition metal layer, and Li still occupies the original position. Liu et al. [16] prepared ternary cathode materials with excellent electrochemical performance for the first time in 1999. Among them, the high capacity of nickel-rich ternary cathode material (more than 60% Ni in the composition) makes it a potential cathode material for the current development of high-energy-density power battery. Therefore, the current research field is mainly focused on the area near the LiNiO$_2$ component. As shown in Figure 1.6, it mainly includes the common LiNi$_{1/3}$Co$_{1/3}$Mn$_{1/3}$O$_2$ (NCM333), LiNi$_{0.5}$Co$_{0.2}$Mn$_{0.3}$O$_2$ (NCM523), LiNi$_{0.6}$Co$_{0.2}$Mn$_{0.2}$O$_2$ (NCM622), and LiNi$_{0.8}$Co$_{0.1}$Mn$_{0.1}$O$_2$ (NCM811). However, these kinds of nickel-rich cathode materials exhibit some drawbacks for the commercialization, including capacity fading during long-term cycling, poor rate capacity, thermal instability, short storage lifetime at elevated temperature, high residual lithium, gas evolution, serious safety concern, Li/Ni cation mixing, and so on. Thereby, some crucial mechanisms are proposed to explain these problems in

Figure 1.6 Phase diagrams of $LiNiO_2$, $LiCoO_2$, and $LiMnO_2$ ternary systems and some representative components. Source: Erickson et al [12]. Reproduced with permission of IOP Publishing.
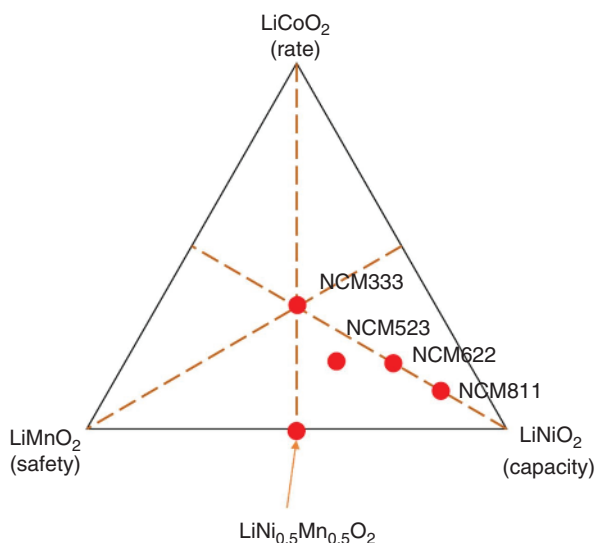
literature: (i) side reaction of electrolyte catalyzed by the delithiated NCM at voltages above 4.3 V with a concomitant oxygen release; (ii) dissolution of the transition metal ions corroded by HF acid from the electrolyte; (iii) layered-to-spinel phase transformation and occurrence of NiO-type phase; (iv) formation of micro-crack and particle fracture originated from internal strain, expansion, and contraction of lattice volume during cycling. The micro-cracks enlarged along the parasitic reaction area between active materials and the electrolyte and accelerated the fracture of particles and decomposition of the electrolyte. Finally, the pulverization of bulk cathode particles occurred. The pulverized and separated particles cannot participate in electrochemical reaction, resulting in the capacity decay (Figure 1.7).

In addition to the common $LiNi_xCo_yMn_{1-x-y}O_2$ (NCM) ternary cathode materials, there is also a special high-capacity ternary cathode material, which is $LiNi_{0.8}Co_{0.15}Al_{0.05}O_2$ (NCA) [18]. The actual specific capacity is as high as 220 mAh g^{-1}. A small amount of Al can stabilize the layered structure. Compared with NCM, NCA has higher structural stability. However, the amphoteric characteristics of Al element make it difficult to synthesize the stable NCA precursor. At present, the NCA cathode materials have been successfully developed by Panasonic in Japan and Tesla in USA, and the energy density of 300 wh kg^{-1} of single cell can be obtained by matching the NCA with silicon/carbon anode.

1.2.2 Spinel-Structured Cathode Materials

$LiMn_2O_4$ with spinel structure belongs to cubic system, and the space group is *Fd*-3*m*. Among them, O atoms are arranged in cubic dense packing, Li ions are in the tetrahedral sites, and Mn occupies half of the octahedral sites (Figure 1.8). Thus, $LiMn_2O_4$ has three-dimensional lithium-ion diffusion channel and excellent rate performance, which is suitable for high-power lithium-ion batteries [19, 20]. The
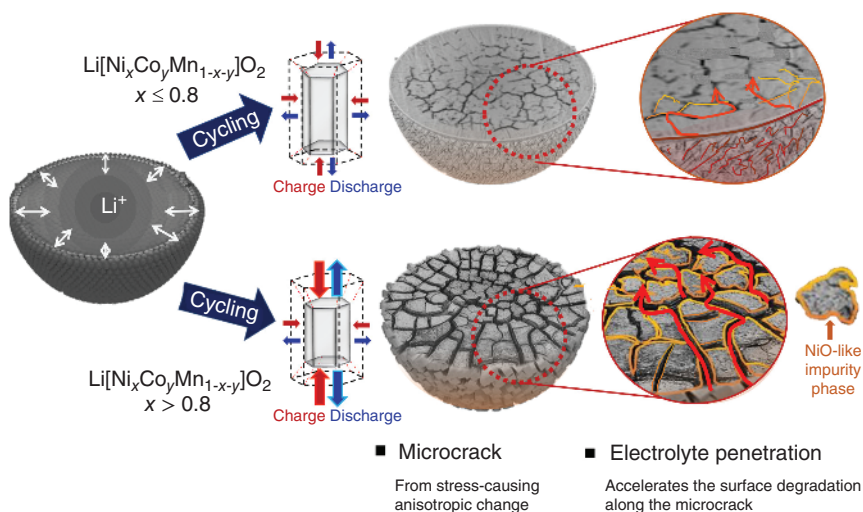
Figure 1.7 Capacity fading scheme of Ni-rich cathode materials. Source: Ryu et al. [17]. Reproduced with permission of American Chemical Society.
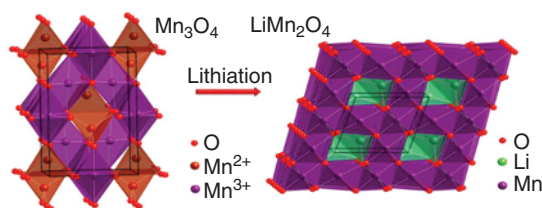

Figure 1.8 Crystal structures of spinel Mn_3O_4 and spinel $LiMn_2O_4$. Source: Adapted from Xia et al [19].

theoretical specific capacity of $LiMn_2O_4$ is 148 mAh g^{-1}, and the working voltage is 4.0 V (vs. Li/Li^+). However, Jahn–Teller distortion caused by entering the octahedron sites of lithium ions will occur during the charging and discharging process, which will affect the reversible capacity and cycle performance of the material. Therefore, the actual specific capacity of $LiMn_2O_4$ can only be 110–120 mAh g^{-1}. In addition, Mn is easy to dissolve in the electrolyte, and the self-discharge will lead to the decline of reversible capacity of the battery.

$LiNi_{0.5}Mn_{1.5}O_4$ can be formed by replacing part of Mn in $LiMn_2O_4$ with Ni. During charging and discharging process, the valence state of Mn in $LiNi_{0.5}Mn_{1.5}O_4$ remains unchanged and only Ni^{2+} and Ni^{4+} change, which will ensure the high structural stability of the materials. At the same time, the working voltage is also increased from the original 4.0 to 4.7 V, which helps to improve the energy density of the battery [21]. According to the different positions occupied by Ni and Mn, $LiNi_{0.5}Mn_{1.5}O_4$ can be divided into *Fd*-3*m* and *P*4$_3$32 space group. In comparison, $LiNi_{0.5}Mn_{1.5}O_4$ with *Fd*-3*m* space group has better structural stability and cycle performance. However, the ordinary organic electrolyte will decompose when the voltage is charged to 4.7 V, resulting in the rapid degradation of the battery capacity deterioration of cycle performance.
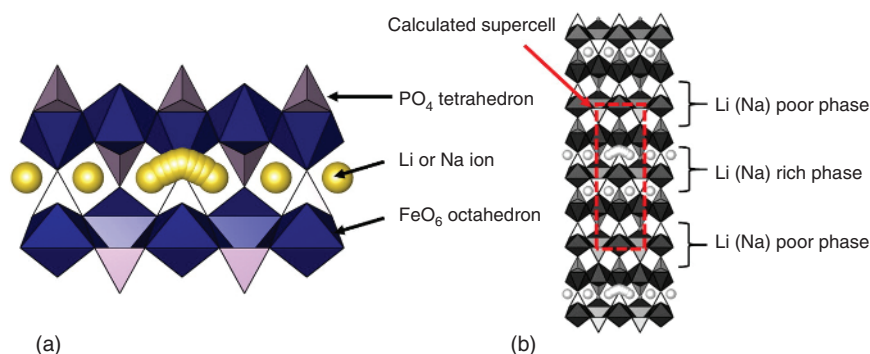
Figure 1.9 Crystal structure diagram of $LiFePO_4$. Source: Nakayama et al [22]. Reproduced with permission of Elsevier.

1.2.3 Olivine-Structured Cathode Materials

Lithium iron phosphate ($LiFePO_4$) with olivine structure has been widely used in power batteries for its excellent cycling performance and safety [22]. It was first reported by Goodenough et al. $LiFePO_4$ of orthorhombic system belongs to the *Pnma* space group, and its theoretical specific capacity is $170 \, mAh \, g^{-1}$, the working voltage is about $3.4 \, V$ (vs. Li/Li^+). During the charging and discharging process, Li^+ occupied in octahedral sites can be transmitted in one-dimensional channel, accompanied by the phase transition of $LiFePO_4$ and $FePO_4$. Due to the strong bonding energy of polyanion PO_4^{3-}, it can still maintain the structural stability when Li ions are completely removed from $LiFePO_4$. However, due to the low ion and electric conductivity of pure $LiFePO_4$, it is necessary to optimize the structure of $LiFePO_4$ for practical application. To sum up, $LiFePO_4$ with low cost and mature synthesis technology is suitable for energy storage system with low energy density requirements (Figure 1.9).

1.3 Anode Materials for LIBs

For cathode materials, the commonly used materials such as lithium cobaltic acid, lithium iron phosphate, and lithium manganate have been well developed, and the capacity is close to the theoretical value. Sulfur and other high-capacity cathode materials are also under development. Therefore, in addition to properly increasing the capacity of cathode materials, people are looking for high-capacity anode materials to replace the traditional graphite anode, which is also one of the most effective strategies to improve the energy density of the lithium-ion battery.

The anode materials of lithium-ion battery can react with lithium ion during the charging process to form lithium-containing compounds, and also lithium ions can be effectively removed during the discharging process. The requirements for an ideal anode material are as follows:
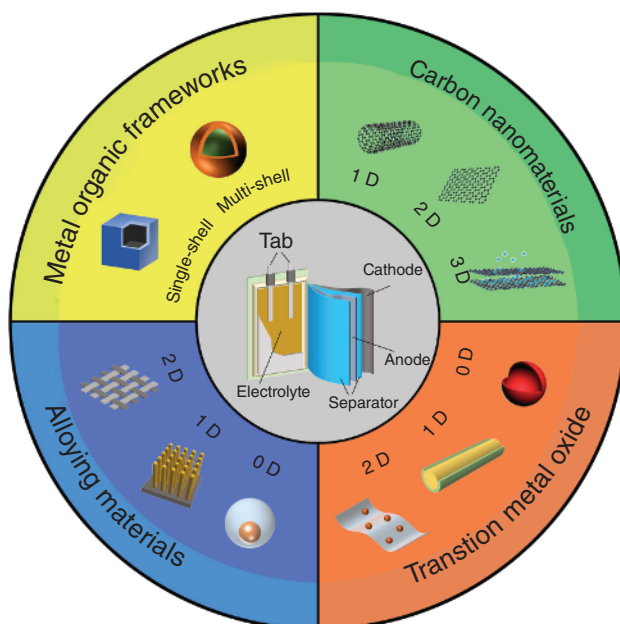
Figure 1.10 Schematic diagram of several representative nanostructured anode materials for LIBs. Source: Cheng et al. [23]. Reproduced with permission of Elsevier.

- low operating voltage;
- high electron and ion transfer rate;
- high capacity;
- high stability

Due to its high stability, graphite with the theoretical specific capacity of $372\,\mathrm{mAh\,g^{-1}}$ is commercially used as anode material, and the actual specific capacity can only be $320–350\,\mathrm{mAh\,g^{-1}}$. With the increasing requirement of the energy density for lithium-ion battery, the low capacity of graphite cannot meet the requirements of the battery. Therefore, newly high-capacity anode materials are highly desired to replace graphite to improve the energy density of the battery (Figures 1.10 and 1.11). According to the mechanism of lithium storage, the anode materials mainly studied at present can be divided into the following three categories: that is, (i) intercalation anode material (lithium ion is reversibly intercalated/exfoliated in the gap between material layers), mainly including common graphite like carbon materials and lithium titanate, (ii) alloy-type anode materials (lithium ion reacts with anode material to form alloy for lithium storage), including silicon, germanium, tin, aluminum, magnesium, etc., and (iii) conversion anode materials (lithium ions react reversibly with metal oxides, nitrides, or phosphates to form metal atoms and lithium-containing compounds including transition metal oxides, sulfides, nitrides, etc.).
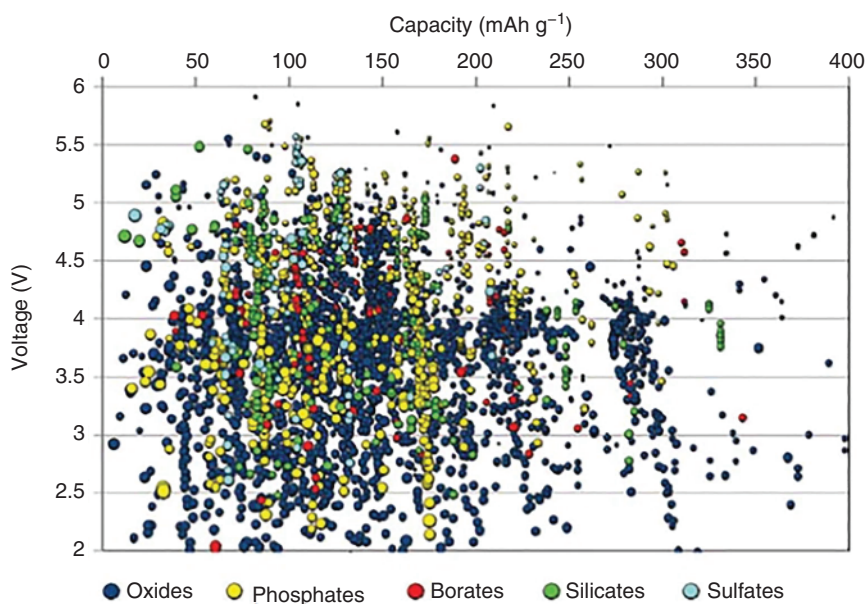
Figure 1.11 The calculated relationship between the LIBs voltage and the theoretical capacity of different compounds for screening materials. Source: Cheng et al. [23]. Reproduced with permission of Elsevier.

1.3.1 Intercalation Anode Materials

Intercalation anode materials mainly rely on the lithium ion diffusion to the gap of layered structure for lithium storage, including carbon-based materials and spinel structured lithium titanate ($Li_4Ti_5O_{12}$). According to the graphite degree of the carbon-based materials, it can be divided into layered graphite, soft carbon, and hard carbon. As a typical carbon, graphite, which mainly includes artificial graphite and natural modified graphite, was commercially used as anode material in 1990s. As shown in Figure 1.12a, during the charging process, lithium ion can be inserted into the interlayer of graphite to form LiC_6, which will impart the graphite with the theoretical specific capacity of $372\,mAh\,g^{-1}$. Meanwhile, the voltage of lithiation platform is low. Due to its excellent cycle stability and low cost, graphite anodes are widely used in commercial lithium-ion batteries. However, the poor compatibility between graphite and organic electrolyte will cause the solvent co-insertion during charging, which affects the performance of the battery. In addition, the lower redox potential of carbon materials (close to that of lithium precipitation) is prone to cause the precipitation of lithium dendrite at a high rate or under the condition of overcharge, which leads to short circuit of battery and serious safety problems.

As shown in Figure 1.12b, three lithium ions can be reversibly intercalated into the spinel structured lithium titanate ($Li_4Ti_5O_{12}$) to form $Li_7Ti_9O_{12}$ phase, and the theoretical specific capacity is $175\,mAh\,g^{-1}$, the working voltage is about
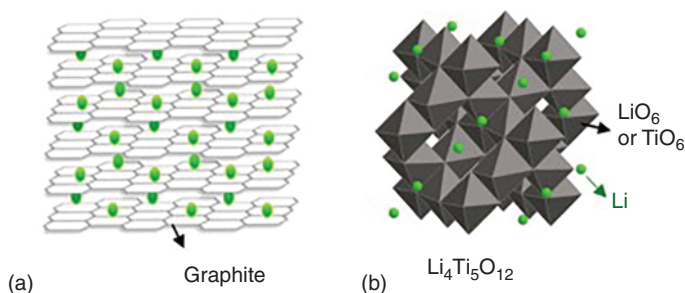
Figure 1.12 Crystal structures of (a) lithiated graphite and (b) $Li_4Ti_5O_{12}$. Source: Nitta et al. [24]. Reproduced with permission of Elsevier.

1.55 V (vs. Li/Li$^+$). The formation of lithium dendrites can be effectively avoided by a higher lithium intercalation/de-intercalation platform, thus improving the safety of battery [25]. At the same time, no structural change of $Li_4Ti_5O_{12}$ occurred during the whole charging and discharging process, and the volume change is less than 0.2%, which is called a "zero strain material" with ultrahigh structural and cyclic stability. However, the poor ions and electric conductivity of $Li_4Ti_5O_{12}$ will result in the poor rate performance of the battery [26]. In general, the intercalation anode materials are of low cost, high safety, and long cycle life. However, the low theoretical specific capacity makes it suitable for energy storage systems with low energy density requirements.

Compared with the ordered materials such as graphite or lithium titanate, amorphous carbon with disordered structure can be thought to be a large number of graphite particles with high crystallinity that are dispersed in the amorphous carbon matrix. Amorphous carbon mainly can be prepared by pyrolysis of the organics at high temperature, and the graphitization degree can be increased with the increase of carbonization temperature. It is worth noting that amorphous carbon can be divided into soft carbon and hard carbon according to the degree of graphitization, as shown in Figure 1.13. Among them, soft carbon refers to the amorphous carbon materials, which can be graphitized above 2000 °C. Soft carbon with low crystallinity, large crystal surface spacing, high irreversible capacity, and good compatibility with electrolyte mainly includes mesophase carbon microsphere, coke, carbon fiber grown in gas phase, and pitch-based carbon fiber, etc. Therefore, soft carbon is generally not directly used as the anode material for lithium-ion battery. Hard carbon refers to the amorphous carbon materials, which are difficult to graphitize even at 3000 °C, and it can be prepared by pyrolysis of polymer (such as polyvinyl alcohol and polyethylene, etc.) and biomass materials (such as shell, animal shell, and cotton, etc.). As anode materials for lithium-ion battery, hard carbon with the high specific capacity of 1000 mAh g^{-1} is favorable for the intercalation of lithium ions without significant expansion of the structure [28]. The layer spacing of amorphous carbon is generally larger than that of traditional graphite, and more lithium ions can be stored in the process of lithium intercalation. In addition, defects in amorphous carbon can absorb lithium ions stably and

Figure 1.13 Schematics of morphologies of graphite, graphitizable carbon (soft carbon), and nongraphitizable carbon (hard carbon). Source: Nishi et al. [27]. Reproduced with permission of John Wiley & Sons.

Graphite

Graphitizable carbon

Non-graphitizable carbon
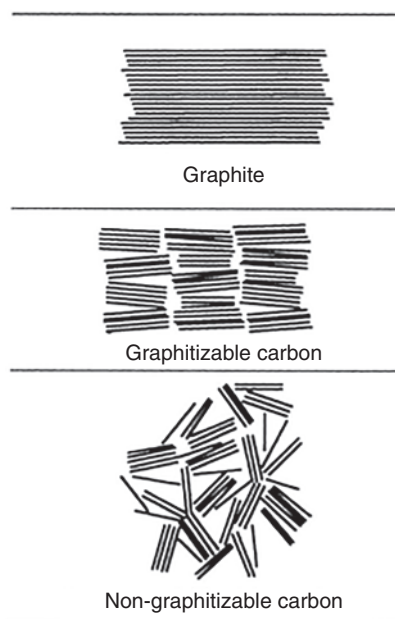
improve the lithium storage performance. In conclusion, amorphous carbon with high capacity possesses a wide range of applications as the anode of lithium-ion batteries.

1.3.2 Alloy Anode Materials

Alloy anode materials mainly include silicon (Si), germanium (Ge), tin (Sn), antimony (Sb), aluminum (Al), and magnesium (Mg). Table 1.1 compares the relevant parameters of alloy anode materials in IVA family and graphite. For C, Si, Ge, and Sn, their fully lithium embedded states are LiC_6, $Li_{4.4}Si$, $Li_{4.4}Ge$, and $Li_{4.4}Sn$, respectively. Compared with carbon-based materials, one atom in the alloy anode can react with many lithium ions and show high capacity. In addition, the alloy anode also has a suitable lithiation/delithiation platform, which is considered to be the most promising alternative anode material to carbon materials for the new generation of battery. For example, Si and Ge can achieve high theoretical specific capacities of 4200 and 1625 mAh g^{-1} by forming $Li_{4.4}Si$ and $Li_{4.4}Ge$ alloys, respectively. However, there are also some problems behind the high capacity of alloy anode materials. Due to the large volume change of active substances during cycling, the active material will be powdered and even peeled off from the current collector and lose electric contact with the conductive network, and the reversible capacity and the cycle stability of the battery will be deteriorated. In addition, the poor conductivity of alloy anode also limits its capacity. In order to realize the commercialization of alloy anode, it is necessary to optimize their structure and composition to improve its electrochemical performance.

Table 1.1 Comparison of Group IVA elements as anode materials for lithium-ion batteries.

Materials	C	Si	Ge	Sn
Bulk density $(g\,cm^{-3})$	2.25	2.33	5.32	7.36
Lithiated phase	LiC_6	$Li_{4.4}Si$	$Li_{4.4}Ge$	$Li_{4.4}Sn$
Theoretical gravimetric capacity $(mAh\,g^{-1})$	372	4200	1625	994
Theoretical volumetric capacity $(mAh\,cm^{-3})$	837	9781	8645	7316
Voltage (vs. Li/Li^+)	0.05	0.4	0.5	0.6
Volume change (%)	12	400	272	259

Source: Liu et al. [29]. Reproduced with permission of Wiley-VCH.

1.3.3 Conversion Anode Materials

The conversion anode materials mainly include oxides, nitrides, phosphates, and sulfides of various transition metals. As an anode material for lithium-ion battery, it has a high theoretical specific capacity and is considered to be a new type of anode material with application prospect. Among the conversion anode materials A_xB_y (A = Co, Fe, Ni, Cu, Mn, Cr, Mo, etc., B = O, S, N, P, etc.), transition metal atom A can react with multiple lithium ions and thus impart the materials with high specific capacity [30]. Take metal oxide A_xO_y as an example, Figure 1.14 shows a schematic illustration of the conversion reaction of transition metal oxides for LIB anodes. From Eq. (1.4), $2y$ lithium ions can be stored per formula unit of metal oxide through a conversion reaction, causing a structural change and amorphization of transition metal oxides that involves large volume expansion. At the end of lithiation, nanoscale transition metal clusters are embedded in the lithium oxide (Li_2O) matrix. During delithiation, these transition metal clusters are oxidized to form amorphous transition metal oxide. The Li_2O, which is inert to lithium, will cause the loss of the first reversible capacity, resulting in the lower initial coulomb efficiency of the material. The high working voltage of these materials (0.5–1.5 V, vs. Li/Li^+) can avoid the formation of lithium dendrites and ensure the high safety of batteries. However, in order to obtain high energy density of battery, it is necessary to match high-voltage cathode materials, which limits the practical application of conversion anode. In addition, A_xB_y anode material is also accompanied by a certain volume change during cycling, which will inevitably cause the collapse and destruction of electrode
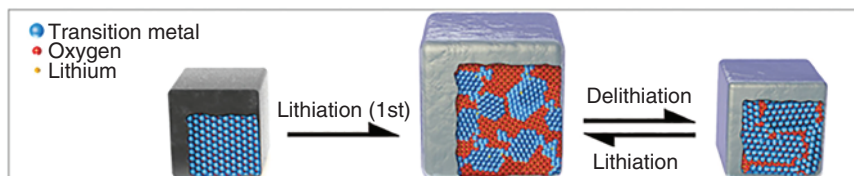

Figure 1.14 Working mechanisms of the conversion anode materials. Source: Yu et al. [31]. Reproduced with permission of John Wiley Sons.

structure, eventually leading to the decline of electrode capacity and the shortening of battery life. It is worth noting that the density of most transition metal elements is relatively high, which will increase the proportion of the anode material in the whole battery and reduce the overall energy density of the battery.

$$M_xO_y + 2y\text{Li}^+ + 2ye^- \leftrightharpoons x\text{M}^0 + y\text{Li}_2\text{O} \text{ (M transition metals)} \tag{1.4}$$
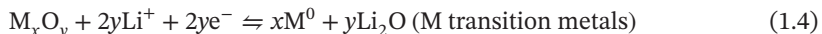
Taking tin oxide (SnO_2) as an example, it is considered as one of the most potential anode materials for the next-generation lithium-ion batteries because of its low operating voltage, high specific and volumetric capacity, high abundance, and low cost [32, 33]. However, the SnO_2-based anode materials suffer from three main issues during the charge/discharge process. The first one is the large volume change (~400%) during the lithiation and delithiation process, resulting in severe electrode pulverization and even peel off from the current collector and thus fast capacity fading during cycling [34, 35]. The second one is the poor electric conductivity of the SnO_2-based anode materials, which will reduce the charge transfer and lead to the low rate capability [36]. The last one is the poor initial Columbic efficiency due to the irreversible conversion reaction during the initial lithiation process, which finally results in the additional cathode material consumption [37, 38]. It is well known that both the conversion reaction and alloying reaction between SnO_2 and Li^+ exist during lithium storage process, as shown below (Eq. (1.6)).

$$\text{SnO}_2 + 4\text{Li}^+ + 4e^- \rightarrow \text{Sn} + 2\text{Li}_2\text{O} \tag{1.5}$$

$$\text{Sn} + x\text{Li}^+ + xe^- \rightarrow \text{Li}_x\text{Sn} \tag{1.6}$$

The conversion reaction (Eq. (1.5)) is partially reversible, while the alloying reaction (Eq. (1.6)) is fully reversible. The common theoretical capacity of SnO_2 anode materials, which can be calculated from the maximum uptake of the Li ions of 4.4 mol per unit of Sn in Eq. (1.6), is 782 mAh g^{-1}. Assuming that Eq. (1.5) is reversible, the capacity contribution from Eq. (1.5) will be 712 mAh g^{-1}, and in this case, the total theoretical capacity of SnO_2 anode materials will reach as high as 1494 mAh g^{-1}. It can be concluded that the electrochemical performance of the SnO_2 anode materials largely depends on the reversibility of the two reactions, and thus it is crucial to improve the reaction reversibility of the reactions during charge/discharge process.

Three strategies can be adopted to solve the above issues (Figure 1.15). One is to encapsulate SnO_2 NPs in robust physical barriers of carbonaceous materials (e.g. amorphous carbon [C], carbon nanotube [CNT], and graphene [Gr], etc.), conductive polymers (e.g. polypyrrole [PPy], polydopamine [PDA], and polyaniline [PANI], etc.), or inorganic materials (e.g. TiO_2, Au, NiTi, vanadium carbide [V$_2$C] MXene). These physical barriers can effectively hinder Sn coarsening by disjoining SnO_2 particles, while simultaneously improving the structural stability and electrical conductivity of the electrodes. Moreover, during the synthesis process, the physical barriers can function as loading matrixes that promote the generation of well-dispersed SnO_2 NPs. The second one is to construct hierarchical, porous, or hollow-structured SnO_2 architectures containing plenty of voids inside the particles
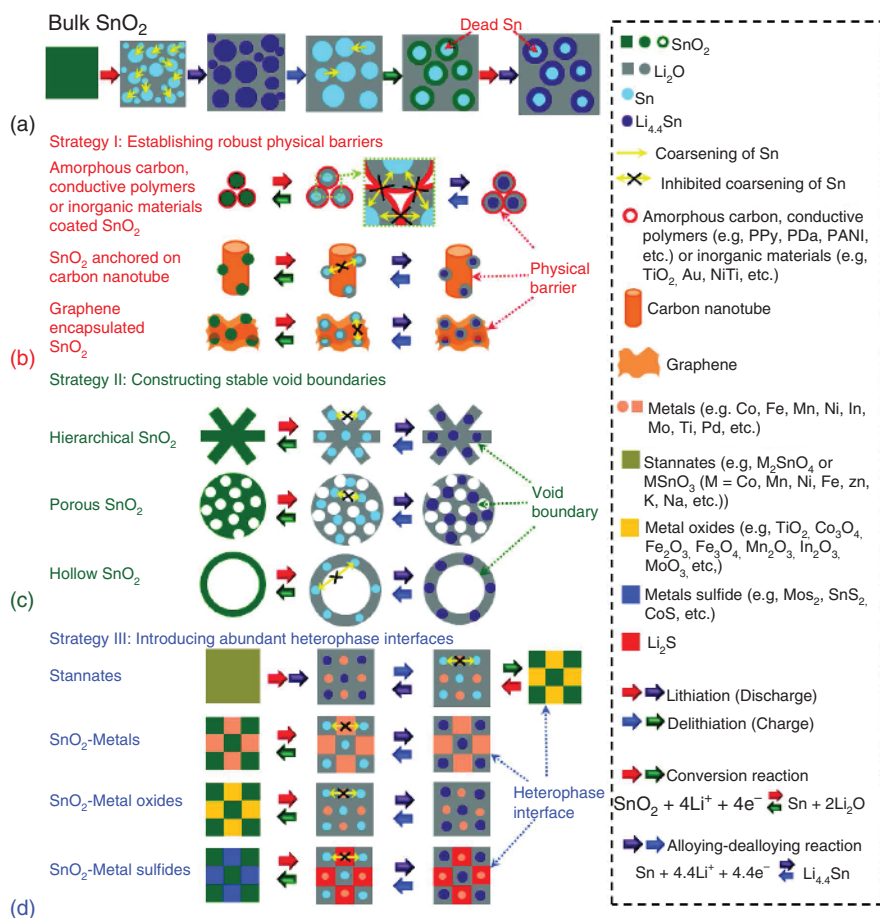
Figure 1.15 Schematic diagram showing the structure evolutions of (a) bulk SnO_2, (b) SnO_2-based nanocomposites with robust physical barriers, (c) hierarchical/porous/ hollow-structured SnO_2 with stable void boundaries, and (d) stannates and heterogeneous materials/SnO_2 hybrids with abundant heterophase interfaces. Source: Zhao et al. [39]. Reproduced with permission of John Wiley Sons.

that divide particles into nanosized subunits separated by high-specific-area void boundaries. The voids not only promote electrolyte infiltration, shortening the lithium transfer distance, but also buffer the volume changes of SnO_2 particles, preventing particle pulverization and stabilizing the void boundaries that hinder Sn coarsening among the divided subunits. The last one is to fabricate stannates (e.g. M_2SnO_4 or $MSnO_3$, M = Mn, Co, Zn, Ba, etc.), doping SnO_2 with metal ions (Mx^+, M = Zn, Fe, In, W, etc.), or mixing SnO_2 with heterogeneous materials (e.g. metals (Ms, M = Au, Co, Pb, Fe, Mn, Ag, etc.), metal oxides, or sulfides (MOs or MSs, M = Co, Fe, Mn, Ni, Cu, Zn, V, Mo, Ti, etc.). The introduced Mx^+, Ms., MOs, or MSs generate abundant heterophase interfaces in cycled SnO_2-based electrodes that divide SnO_2 into individual nanocrystalline domains and impede Sn coarsening

between the isolated SnO_2 domains. Furthermore, some transition metal elements (e.g. Co, Fe, Ni, Mn, etc.) that exhibit high conversion reaction reversibility with Li_2O can promote the decomposition of Li_2O and facilitate the reverse conversion reaction from Sn and Li_2O to SnO_2, improving the capacity.

1.3.4 Lithium Metal Anode

Lithium metal anode has been thought to be the holy grail to realize the highest energy density owing to the high theoretical capacity (3860 mAh g^{-1}, about 10 times that of the graphite anode) and the low electrochemical potential (-3.04 V vs. the standard hydrogen electrode) of Li metal anode [40–42]. Nevertheless, Li dendrites formed during cycling hinder the development of lithium metal anode, which leads to low Columbic efficiency, poor cycle stability, and even short-circuiting-related safety hazards [43, 44]. As illustrated in Figure 1.16, the lithium foil contacts and reacts with electrolyte to form a solid electrolyte interface (SEI) during cycling due to its high activity, and the SEI between the lithium and electrolyte is inhomogeneous and relatively fragile. In the stage of lithium deposition, Li$^+$ ions are more likely to deposit on the bumps located on the surface of the lithium foil due to the accumulation of electrons, forming dendritic lithium metal. The generation of dendrites and the volume change of the electrode during cycling lead to the rupture of the SEI, and the fresh lithium is again exposed to the electrolyte and reacts with it to form new SEI. This process continues throughout the battery cycling, constantly consuming electrolyte and lithium, resulting in low Columbic efficiency. The lithium dendrites may break from the matrix and be wrapped by the SEI [45], accompanied by losing their activity and forming "dead lithium," at the same time, the SEI also becomes thicker and thicker, resulting in higher and higher interface resistance. More seriously, the gathering of dendrite is highly possible to pierce the membrane, causing a short circuit inside the battery, leading to ignition or explosion
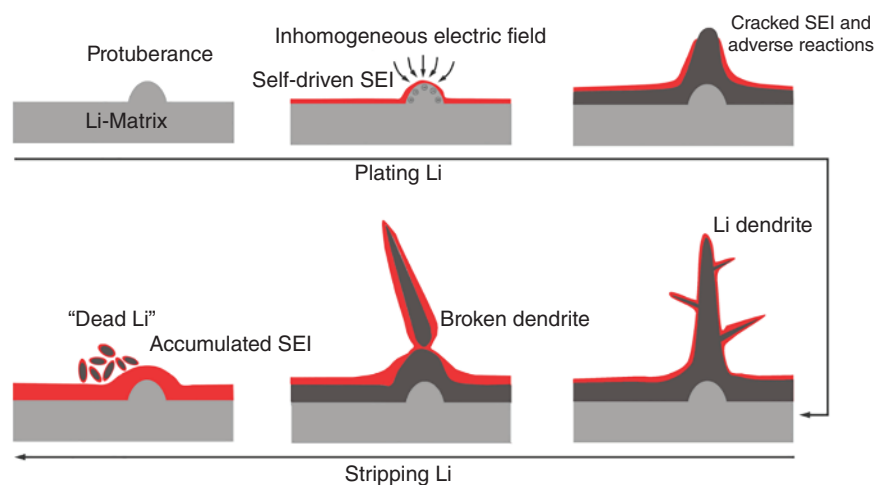

Figure 1.16 Scheme of dilemma for Li metal anode in rechargeable batteries.
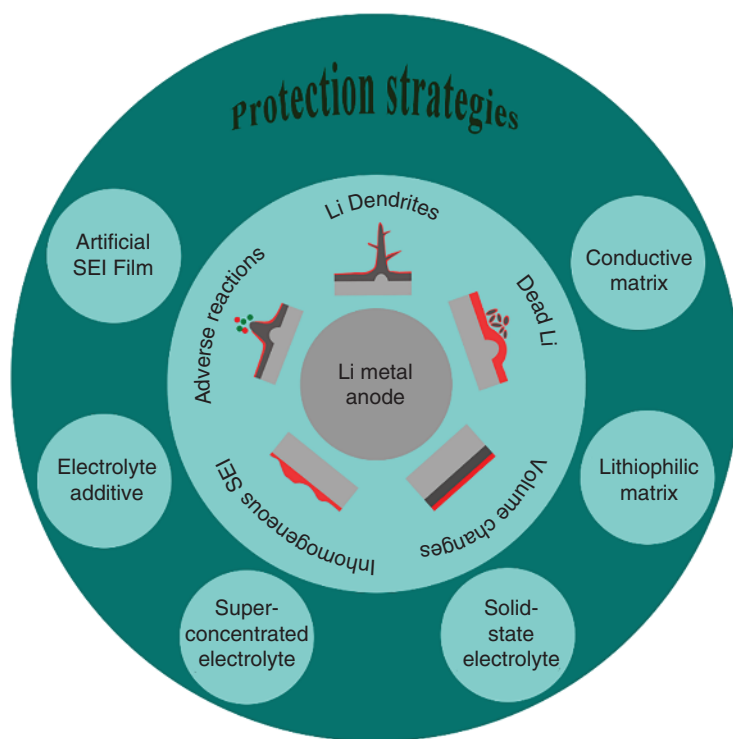
Figure 1.17 Solutions for Li metal anode in rechargeable batteries.

of the battery. Therefore, suppressing dendrite growth and mitigating electrode's volume change are fundamental methods for improving the performance of lithium metal anode [46–51].

According to previous reports, the current strategies for addressing the issues of lithium metal anodes are as follows (Figure 1.17): (i) designing a stable and uniform artificial SEI to replace the fragile native SEI, and thus achieving homogeneous Li deposition [52, 53]; (ii) developing electrolyte additives to help uniform Li deposition or stabilize SEI [54–56]; (iii) employing high-modulus solid-state electrolyte (SSE) to inhibit the growth of lithium dendrites [57–59]; (iv) replacing lithium metal with lithium alloy to suppress dendritic lithium formation [60, 61]; (v) constructing novel structured Li metal anode by nanotechnology to regulate Li ions plating/stripping behavior and mitigate the volume change during repeated cycling [62–65]. Each of the above methods has its advantages and disadvantages. For example, although the artificial SEI cannot reduce the overall energy density of the batteries, most of them are not strong enough to withstand the constant volume change and may be ruptured after a long cycling. Adding additives into electrolyte is easy to operate on a large scale; however, those additives will be continuously consumed during cycling. SSEs are considered particularly promising because of their inherent safety characteristics and potential to prevent dendritic deposition of the lithium, while

the problems of low ionic conductivity and large interfacial impedance hinder the commercialization of SSE [66]. Alloyed anodes can efficiently suppress the Li dendritic formation, but they will increase the mass of the electrode, resulting in lower energy density of battery. Structured anodes can improve the performance of lithium metal anode in several aspects, but they should present good mechanical properties, and almost all of them meet the trouble of severe interfacial side reactions.

1.4 Electrolyte

The electrolyte acts as a bridge between cathode and anode to transport Li^+. The basic requirements of electrolyte with excellent performance include: (i) high ionic conductivity and low viscosity; (ii) low melting point, high boiling point, and wide temperature range; (iii) wide electrochemical window and good chemical stability; (iv) good compatibility with positive and negative materials. The above requirements are necessary for the electrolyte to work continuously and stably in the lithium-ion battery and guarantee the high performance of the lithium-ion battery [13]. The compatibility between electrolyte and cathode and anode will also affect the performance of lithium-ion battery. The reduction of electrolyte on the surface of carbon anode results in the formation of solid electrolyte interface, referred as SEI film. The oxidation reaction on the surface of metal oxide leads to the formation of cathode electrolyte interface film, which is referred as CEI film. The formation of stable interfacial film is conducive to improve the cycle stability of batteries.

1.4.1 Liquid Electrolyte

The electrolyte consists of lithium salt, solvent, and functional additive, and the three components and their working principles are described in detail below.

1.4.1.1 Lithium Salts

Lithium salt mainly provides a large amount of Li^+ for electrolyte, but its anion is also an important factor affecting the physical and chemical properties of electrolyte. Proper lithium salt can effectively improve the energy density, broaden the electrochemical window, improve the cycle life of the battery, and broaden the working temperature range of the electrolyte. Lithium salt should exhibit the following characteristics: (i) it is easy to dissolve in organic solvent with high solubility; (ii) it is easy to ionize, so that the electrolyte can be highly ionic conductive; (iii) good thermal stability and not easy to decompose; (iv) good oxidation–reduction stability; (v) noncorrosive to Al and Cu collector; (vi) easy to prepare, low cost, environmentally friendly. At present, the widely used lithium salts mainly include $LiPF_6$, $LiBF_4$, lithium hexafluoride arsenate ($LiAsF_6$), lithium perchlorate ($LiClO_4$), and other inorganic salts, as well as the organic lithium salts such as LiBOB, LiODFB, lithium trifluoromethylsulfonate ($Li(CF_3SO_3)$), and lithium trifluoromethylsulfonimide [LiTFSI]) [67–69].

(1) $LiPF_6$. At present, the commercial lithium salt is mainly $LiPF_6$, which possesses the following advantages: high solubility and conductivity; effective film formation on the electrode surface; passivation of the positive collector to prevent its dissolution; wide electrochemical stability window. However, the thermal stability of $LiPF_6$ is poor, and it is easy to decompose into PF_5 and LiF at high temperature, and the decomposition products are easy to hydrolyze to produce HF, which will damage the structure and performance of the battery and pollute the environment [70].

(2) $LiBF_4$. $LiBF_4$, which exhibits higher thermal stability than $LiPF_6$, is not sensitive to water and is not easy to generate HF. It has small charge transfer impedance at low temperature. It is the most widely used lithium salt in industry except $LiPF_6$ [71]. Compared with $LiPF_6$, $LiBF_4$ has a small anion radius and is easy to associate, so its solubility in organic carbonate solvent is low and its conductivity is not high. Moreover, $LiBF_4$ has a poor film-forming property and poor compatibility with the electrode, so it is usually used in combination with other lithium salts [72].

(3) LiBOB. LiBOB is a new type of boron-based lithium salt. Due to its excellent performance, its research is more in-depth. LiBOB has high decomposition temperature, good thermal stability, easy to form film on the negative electrode surface, and has a good passivation effect on Al collector [70]. The lithium-ion battery with LiBOB can be cycled well at 60 and 70 °C, while lithium-ion battery with $LIPF_6$ cannot work under the same conditions [67]. LiBOB is mainly sensitive to water, and its solubility in common carbonate solvent is small. Although it is easy to form a film, its impedance is large, which seriously affects the low-temperature performance and rate performance of the battery [69]. It is rarely used alone and is generally used as an additive.

(4) LiODFB. LiODFB is another new type of boron-based lithium salt. It combines the structure and advantages of LiBOB and $LiBF_4$. LiODFB is not only similar to LiBOB, but also can form stable SEI film on the anode surface. Compared with LiBOB, the SEI film formed by LiODFB has smaller impedance and higher stability [73]. LiODFB can passivate aluminum foil and inhibit the oxidation of electrolyte, so it has good compatibility with cathode materials. However, the high impedance of LiODFB at low temperature limits its application at low temperature.

(5) LiTFSI. Because of its high conductivity (comparable to $LiPF_6$) and high thermal decomposition temperature (>360 °C), the stable interfacial film on the cathode surface and low charge transfer resistance at low temperature can be obtained. It has attracted wide attention in the field of high and low-temperature batteries [74]. However, LiTFSI is corrosive to the current collector.

1.4.1.2 Organic Solvent

The properties of organic solvents also affect the properties of electrolyte. The following properties should be considered in the selection of solvents for wide-temperature electrolyte: (i) high flash point and low vapor pressure, which are related to the safety

Table 1.2 Some physical properties of organic solvents.

	Statue	Solvent	Melting point (°C)	Boiling point (°C)	Flash point (°C)	Dielectric constant (25 °C)	Viscosity (25 °C)	D.N.	A.N.
Carbonate	Ring	EC	36.4	248	150	89.78	1.90 (40 °C)	16.4	
		PC	−48.8	242	135	64.92	2.53	15.1	18.3
		BC	−53	240		53	3.2		
		VC	22	162	73				
	Chain	DMC	4.6	91	15	3.107	0.59 (20 °C)	16	
		DEC	−74.3	126	33	2.805	0.75	14.6	
		EMC	−53	110	23	2.958	0.64		
Carboxylate	Ring	γBL	−43.5	204	101	39	1.73	18	18.2
	Chain	EA	−84	77	−4	6.02	0.45	17	
		MF	−99	32	−32	8.5	0.33		
		MA	−98	57		6.7	3.64	16.5	
		PA	−92.5	101.6	14				
		EP	−73.9	99.1	12.2		0.9 (15 °C)		
		MB	−84	102	11		0.6		

EC: Ethylene carbonate, PC: Propylene carbonate, BC: Butene carbonate, VC: Vinyl carbonate, DMC: Dimethyl carbonate, DEC: Diethyl carbonate, EMC: Ethyl carbonate, γ BL: γ-butyrolactone, EA: Ethyl acetate, MF: Methyl formate, MA: Methyl acetate, PA: Propyl acetate, EP: Ethyl propionate, MB: Methyl butyrate.

of the battery at high temperature; (ii) low melting point and high boiling point, the solvent is in a liquid state in a wide temperature range; (iii) high dielectric constant, which is favorable for the dissolution of lithium salt and ionize into free ions; (iv) wide electrochemical window. At present, the main solvent used in the electrolyte of lithium-ion battery is carbonate solvent. The common organic solvents are listed in Table 1.2.

Carbonate mainly includes two types, that is, ring carbonate with high dielectric constant and viscosity, and chain carbonate with low dielectric constant and viscosity. Carbonate solvents are widely used in lithium-ion batteries because of their good electrochemical stability, high flash point, and low melting point. The ring carbonate solvents (EC and PC) with a higher dielectric constant and flash point can effectively dissolve and ionize lithium salts. EC is an indispensable component in electrolyte solvent system because of its good film-forming property. The ionic conductivity of EC is higher than that of the corresponding PC-based electrolyte, but EC is a solid at room temperature, which is often mixed with chain carbonate (mainly DMC, DEC, and EMC [Ethyl carbonate]) with lower melting point; however, the low-temperature performance of the electrolyte system containing EC is

poor. The lower melting point of PC can widen the lower temperature limit of electrolyte. However, PC and Li^+ are easy to be co-embedded into graphite. In general, PC needs to be used together with solvents with good film-forming properties, such as EC, or film-forming additives. It can be seen from the data in Table 1.2 that the polarity of the solvent with high dielectric constant is larger, which is conducive to the dissolution and ionization of lithium salt, meanwhile, the viscosity and melting point of the solvent are often high, which will affect the low-temperature performance of the electrolyte, while the relative dielectric constant of the solvent with low viscosity is also lower. Therefore, it is not easy to meet all the requirements of electrolyte for one solvent. Generally, the ring carbonate and chain carbonate are used together to widen the application temperature range of electrolyte.

Due to the low oxidation potential of ether-based electrolyte, it is rarely used in lithium-ion batteries. Sulfone solvents are often used in high-voltage batteries because of their wide electrochemical window. However, the melting point of sulfone is generally high, so it cannot be used in wide-temperature electrolyte system. Carboxylate solvent has low melting point and can be used as a cosolvent in low-temperature electrolyte system [75]. However, carboxylate with low flash point and high vapor pressure may reduce the safety of electrolyte at high temperature, which is not suitable for wide-temperature electrolyte [76].

1.4.1.3 Functional Additives

Additives are also one of the essential components in the electrolyte system and are considered to be the most economical and effective component to improve the cycle performance and life of the battery. The amount of additives, whether calculated by mass or volume fraction, shall not exceed 5%. There are many kinds of electrolyte additives, such as lithium salt, solvent, and even polymer. According to its function, it can be divided into anode film-forming additive, cathode film-forming additive, anti-overcharge and overdischarge protection additive, and flame retardant additive. The film-forming additives of electrodes affect the interface properties between the electrolyte and the electrode.

(1) Anode film-forming additive. During the first charge of the battery, the electrolyte will reduce and decompose on the surface of anode, thus forming SEI film on the surface of anode. PC is an ideal solvent for widening the lower temperature limit of electrolyte because of its low melting point. However, PC and Li^+ are easy to be co-embedded between graphite layers, so it is necessary to add film-forming agent to form stable SEI membrane.

At present, vinyl carbonate (VC) is widely used as anode film-forming additive, due to the unsaturated C=C double bond in VC molecular structure and the lower energy of the lowest space orbit (LUMO), which can preferentially reduce the electrolyte, form a stable SEI film, and improve the capacity of cell. It is reported that the initial capacity of cell can be increased from 208 to 334 $mAh\,g^{-1}$. It is shown that the mechanical properties of SEI film can be improved by adding VC in the electrolyte [76]. Fluoroethylene carbonate (FEC) is also a commonly used anode film-forming additive [77]. F atom can

be introduced into EC to form C—F bond by adding FEC. Due to the strong electron absorption ability of C—F bond, the LUMO energy of FEC is lower than that of EC. Similar to VC, FEC can preferentially reduce to form stable and low-impedance SEI film, so as to improve the compatibility between electrode and electrolyte.

Boron compounds have been extensively studied because of their ability to improve the interfacial membrane of the battery. For example, the LiBOB mentioned above also has the advantage of low LUMO energy than that of organic carbonates, which can be used as an additive to give priority to film formation, inhibit the decomposition of electrolyte, and stabilize the interface impedance. LiODFB formed by introducing F atom with stronger electronegativity to LiBOB has similar film-forming performance with LiBOB, and SEI film with higher stability and lower impedance can be formed on the surface of anode [78].

(2) Cathode film-forming additive. When Li^+ is embedded/removed from the cathode materials, the valence state of the central transition metal atom will change, which makes the lattice constant change. During the charging process, when a large amount of Li^+ comes out of the cathode, the change of lattice constant may lead to the phase transformation of crystal structure and even destroy the crystal structure, resulting in the dissolution of metal ions. The electrolyte will be oxidized and decomposed under the catalysis of transition metal ions at high potential. Therefore, in order to protect the stability of the cathode materials, the cathode film-forming additive should also be added. The formation mechanism of CEI film is that the electrolyte is oxidized on the surface of cathode. According to this mechanism, as long as the molecules with higher energy of the highest electron occupied orbit (HOMO) than that of the electrolyte solvent are selected and added to the electrolyte, they will be preferentially oxidized, so as to improve the compatibility between the electrolyte and cathode.

It has been reported that biphenyl and thiophene possess high orbital energy (HOMO) and are prone to oxidative decomposition. The capacity retention of $LiCoO_2$ cells can be significantly improved by adding 0.1% biphenyl and thiophene [79]. It is shown that biphenyl and thiophene can form interfacial film on the surface of cathode, which will inhibit the oxidation decomposition of the electrolyte and improve the cycle performance of the battery. In addition, LiBOB and LiODFB can also help to form film on the surface of cathode, finally improving the cycling performance of the battery [80].

1.4.2 Solid Electrolyte

Solid electrolyte, also known as fast ionic conductor or super ionic conductor [67], can be divided into polymer electrolyte and inorganic solid electrolyte (Figures 1.18 and 1.19). According to crystalline state, it can be divided into crystalline electrolyte and amorphous electrolyte. Crystalline electrolyte refers to inorganic solid electrolyte, while amorphous electrolyte includes polymer electrolyte and glassy inorganic solid electrolyte. The solid electrolyte for lithium-ion battery should meet

Figure 1.18 Reported total lithium-ion conductivity (unless otherwise mentioned) as a function of temperature. Source: Bachman et al. [81]. Reproduced with permission of American Chemical of Society.

Figure 1.19 Reported total ionic conductivity of solid-state lithium-ion conductors at room temperature. Source: Bachman et al. [81]. Reproduced with permission of American Chemical of Society.

the following requirements [82]: good lithium-ion conductivity; very low electronic conductivity; no or very small grain boundary resistance; good chemical stability, no reaction with electrode materials and Li; high electrochemical decomposition voltage; green environmental protection, low price and easy to prepare.

1.4.2.1 Polymer Electrolyte

Polymer electrolyte is a kind of polymer/lithium salts composite, which is based on the amorphous structure of PEO, polyvinyl butyral (PVB), polyacrylonitrile (PAN), polyvinylidene fluoride (PVDF), polymethylmethacrylate (PMMA), and so on. The conductivity comes from the migration or transition of lithium ions in the spiral channel formed by polymer chain (Figure 1.20). At the early stage, the polymer electrolytes were mainly formed by PEO and alkali metal salts, and the ionic conductivity was only 10^{-8} S cm^{-1} [84]. Later, the researchers found that the room temperature conductivity of the material was obviously improved to 10^{-4}–10^{-3} S cm^{-1} by introducing the organic solution into polymer electrolyte to form gel polymer electrolyte [85, 86]. Decreasing the glass transition temperature and increasing the number of carrier (Li$^+$) are the main ways to improve the ionic conductivity of materials, include doping, adjusting polymer structure, organic solvent plasticizing, and changing the structure and concentration of lithium salt [86]. However, due to its poor thermal stability and mechanical properties, its development and application are seriously limited.

1.4.2.2 Li$_3$N and its Derivatives

Li$_3$N is the first reported inorganic solid electrolyte with high ionic conductivity at room temperature. Its crystal structure is hexagonal system, which contains Li$_2$N layer and pure Li layer perpendicular to the *c* axis (Figure 1.21). The conductivity of Li$_3$N crystal is anisotropic. The conductivity of ions perpendicular to the *c*-axis
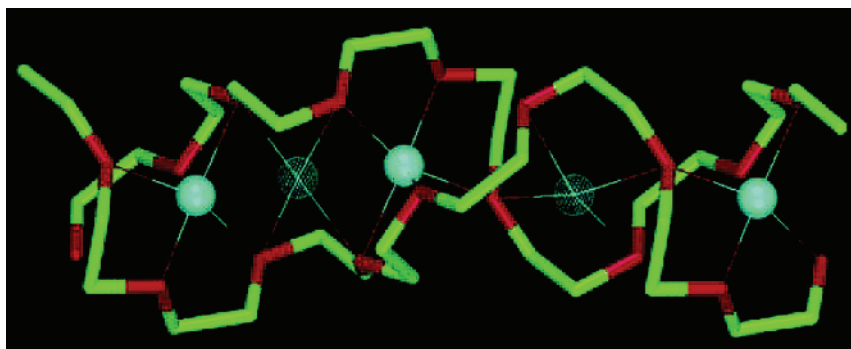

Figure 1.20 Schematic diffusion pathway of the Li$^+$ cations in PEO$_6$:LiPF$_6$. Thin lines indicate coordination around the Li$^+$ cation; solid blue spheres, lithium in the crystallographic five-coordinate site (note that the fifth thin line is very short in this view); meshed blue spheres, lithium in the intermediate four coordinate sites; green, carbon; red, oxygen. Source: Stoeva et al. [83]. Reproduced with permission of American Chemical Society.
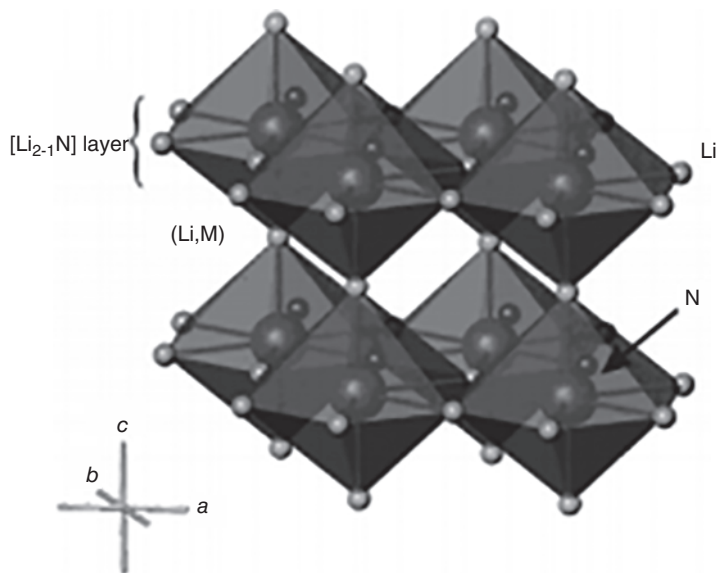
Figure 1.21 Structure of $Li_{3-x-y}M_xN$. Polyhedral representation showing layers of edge-sharing $NLi_6(Li, M)_2$ hexagonal bipyramids linked by vertexes along the *c* axis. Source: Gregory et al. [87]. Reproduced with permission of American Chemical Society.

can reach 10^{-3} S cm^{-1}, but the conductivity parallel to the *c*-axis is very low. The decomposition voltage of Li_3N is only 0.45 V, and its chemical stability is poor (sensitive to air and flammable in water, etc.), which seriously limits its practical application. In order to improve the performance of Li_3N, LiX (X = Cl^{-1}, Br^{-1}, I^{-1}) was added to form Li_3N–LiX eutectic. The stability and decomposition voltage of Li_3N–LiX eutectic were improved obviously (>2.5 V), but the ionic conductivity decreased to 10^{-5}–10^{-6} S cm^{-1}. The conductivity of $Li_9N_2Cl_3$ was improved by replacing part of Li$^+$ with metal cations such as Na$^+$, K$^+$, Rb$^+$, CS$^+$, Mg^{2+}, Ba^{2+}, and Al^{3+} [87].

1.4.2.3 Perovskite Solid Electrolyte

The general structural formula of perovskite solid electrolyte is $Li_{3x}La_{2/3-x}TiO_3$ ($0.04 < X < 0.17$, LLTO) (Figure 1.22) [88]. $Li_{0.34}La_{0.51}TiO_{2.91}$ with the room-temperature ionic conductivity of 10^{-3} S cm^{-1} was successfully synthesized by Ingaguma and Chen Liquan et al. Although this kind of material has high ionic conductivity, when contacting with Li, Ti^{4+} in the structure is reduced to Ti^{3+}, it makes the material to show high electronic conductivity and become a mixed conductor of electrons and lithium ions, leading to the failure of battery, which seriously limits its practical application. The properties of the electrolyte materials can be improved by substitution of some elements. For example, Sr^{2+} is used to replace part of Li$^+$ and La^{3+} in the structure of ABO_3, the vacancy concentration of Li is increased, the cell volume is increased, and the bottleneck of Li$^+$ transport is enlarged. The bulk lithium ionic conductivity at 25 °C can be as high as 1.5×10^{-3} S cm^{-1}, while the
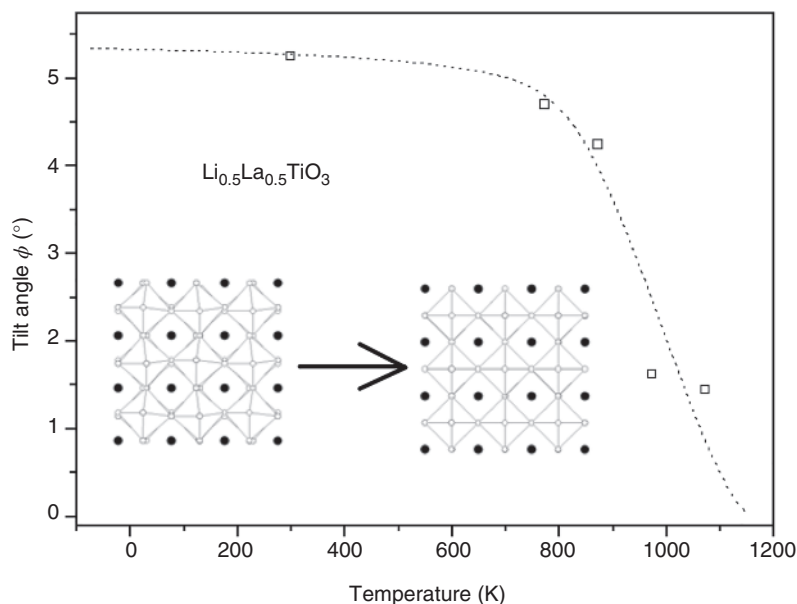
Figure 1.22 Structure of perovskite solid electrolyte. Source: Varez et al. [88]. Reproduced with permission of American Chemical Society.

total conductivity is $5.5 \times 10^{-4}\,\mathrm{S\,cm^{-1}}$ [89]. The properties can also be improved by doping at B position with metal elements (SN, Zr, Mn, Ge, Al, etc.).

1.4.2.4 LISICON

$Li_{14}Zn(GeO_4)_4$ reported by Hong at Massachusetts Institute of technology is the first LISICON (lithium super ionic conductor) compound. The ionic conductivity can reach $0.13\,\mathrm{S\,cm^{-1}}$ at $300\,°C$ and $\sim10^{-7}\,\mathrm{S\,cm^{-1}}$ at room temperature. Then, Bruce and West studied the properties of $Li_{2+2x}Zn_{1-x}GeO_4$ [90]. LISICON can be considered as the solid solution of Li_4GeO_4 and Zn_2GeO_4, and the structure is similar to that of γ-Li_3PO_4. At the same time, the solid solutions of Li_4XO_4 (X = Si, Sc, Ge, Ti) and Li_3YO_4 (Y = P, As, V, Cr), with the general formula of $Li_{3+x}Y_{1-x}X_xO_4$, have also been studied (Figure 1.23) [91, 92]. The volume of crystal cell increased significantly by substituting O^{2-} with S^{2-} of larger radius, and the size of ion transport channel was increased, in addition, the binding of structural framework to Li^+ was weakened due to the strong polarity of S^{2-}, making the conductivity of Li_2S–GeS_2–P_2S_5 reach $10^{-3}\,\mathrm{S\,cm^{-1}}$, which is equivalent to that of liquid organic electrolyte [93, 94].

1.4.2.5 NASICON

NASICON is the sodium fast ionic conductor, which firstly refers to solid solution of $Na_{1+x}Zr_2Si_xP_{3-x}O_{12}$ (x = 2), $Li_3Zr_2Si_2PO_4$ was obtained by replacing Na^+ in the structure with Li^+; however, due to the larger radius of Na^+ than that of Li^+, its ionic conductivity is very low (Figure 1.24). The channel that is suitable for Na^+ transportation is too large for Li^+ [96, 97]. Based on this, the $LiTi_2(PO_4)_3$ was obtained
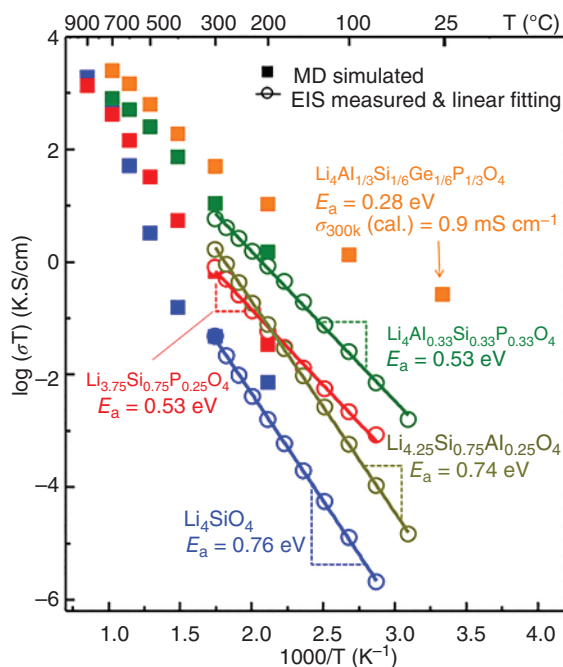
Figure 1.23 Li$^+$ ionic conductivity (σ), Arrhenius plots for Li$_4$SiO$_4$ (blue), Li$_{3.75}$Si$_{0.75}$P$_{0.25}$O$_4$ (red), Li$_{4.25}$Si$_{0.75}$Al$_{0.25}$O$_4$ (dark yellow), Li$_4$Al$_{0.33}$Si$_{0.33}$P$_{0.33}$O$_4$ (green), and Li$_4$Al$_{1/3}$Si$_{1/6}$Ge$_{1/6}$ P$_{1/3}$O$_4$ (orange). MD simulated values are shown in solid squares. Conductivity values deduced from electrochemical impedance spectroscopy (EIS) measurements are shown in circles. Linear fits for experimental values are plotted in solid lines. The activation energies are derived in the temperature range of 50–300 °C. Source: Deng et al. [90]. Reproduced with permission of American Chemical Society.

by replacing Zr^{4+} in the structure with Ti^{4+} with a smaller ion radius, and the ionic conductivity was significantly improved. In addition, Ti^{4+} can be replaced by Al^{3+}, In^{3+}, Ga^{3+}, La^{3+}, and Y^{3+}, which can also effectively improve the ionic conductivity of the material. It is difficult to obtain single dense phase of the solid electrolyte with NASICON structure. The large resistance of the grain boundary is an important factor for the low conductivity of the material. Moreover, the poor chemical compatibility between NASICON and lithium must be overcome before commercialization.

1.4.2.6 Garnet

Li$_5$La$_3$M$_2$O$_{12}$ (M = Ta, Nb) with garnet structure found by Thangadurai and weppner et al. [98] is another type of lithium-ion solid electrolyte. Figure 1.25 shows the crystal structure of Li$_5$La$_3$M$_2$O$_{12}$ [99], which belongs to the cubic system, and the space group is *Ia*-3*d*. At room temperature, it has high conductivity of ~10^{-6} S cm^{-1} [100] and high decomposition voltage (6 V vs. Li/Li$^+$). In the garnet crystal structure, lithium ions occupy tetrahedral and octahedral positions, respectively, while tetrahedron and adjacent octahedron are coplanar. When the transition lithium ions enter the tetrahedron sites, due to coplanar connection, the lithium ions will generate

Figure 1.24 Structures of NASICON polymorphs: (a) orthorhombic (Pbna), (b) monoclinic (P2$_1$/c), (c) triclinic, and (d) Corundum-like. Source: Anantharamulu et al. [95]. Reproduced with permission of Springer Nature.

(a)

(b)

(c)

(d)
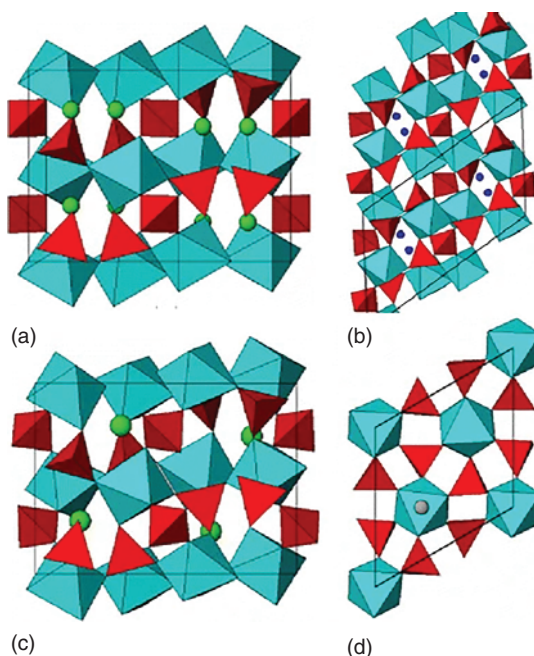
strong electrostatic repulsion with the lithium ions at the octahedron site, thus, part of the lithium ions at the octahedron site will transport to the tetrahedral position or octahedral position connected by common edges, and the above lithium ion will interact with the adjacent lithium ions, thus forming a so-called synergistic effect, and finally lithium ions can migrate rapidly in the crystal by this synergistic effect. The ionic conductivity of the materials can be improved by substitution of La^{2+} with Ca^{2+}, Sr^{2+}, Ba^{2+}, Eu^{3+}, K^+, or M with In^{3+}, Zr^{4+}, Gd^{3+}, and Y^{3+} [101, 102].

1.4.2.7 Glassy Inorganic Solid Electrolyte

Amorphous fast ionic conductor, also known as ionic conducting glass, is characterized by a long-range disordered structure of rigid skeleton. Compared with the crystal fast ionic conductor, the amorphous state itself belongs to the high defect structure, which is conducive to the migration of ions. The chemical composition is continuously adjustable, which makes it easy to explore and find new materials in a wide range of components. The macroscopic properties are isotropic, the preparation and processing are relatively simple, and the production cost is low. On the other hand, like other amorphous materials, there are inherent disadvantages, such as thermodynamic instability, spontaneous crystallization, and so on.

Glass itself belongs to an irregular network structure with different sizes of channels, which is easy to block cations with larger radius, while for lithium ions with smaller radius, conduction in the glass network will not be blocked. Therefore, the conductivity of glassy solid electrolyte is high, which can reach 10^{-3} S cm^{-1} at room temperature. However, due to its metastable state, it is unstable at high temperature and easy to crystallize, which will decrease the strength and conductivity of the
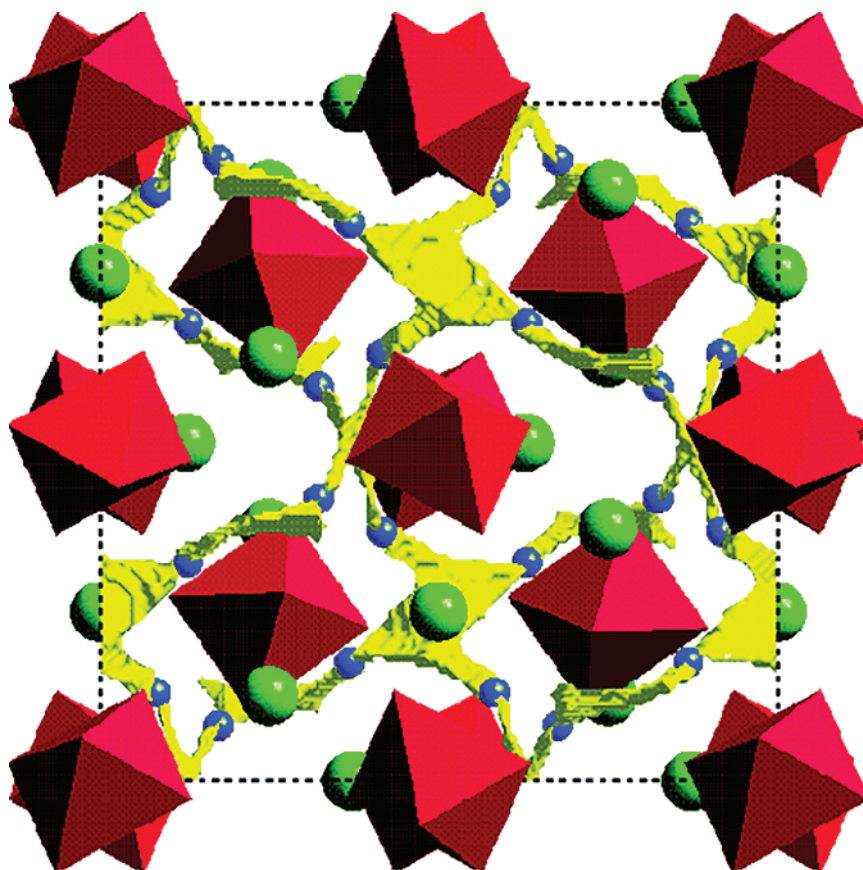
Figure 1.25 Crystal structure of garnet-like $Li_5La_3M_2O_{12}$ (MO_6: octahedral, lanthanum: large solid circles; Li(I): empty circles; Li(II): small solid circles). The lithium's oxygen coordination environment is shown on the right-hand side. Source: Thangadurai et al. [98]. Reproduced with permission of American Chemical Society.

material. At present, glass-based inorganic lithium-ion solid electrolyte is mainly divided into oxide glassy electrolyte and sulfide glassy electrolyte.

The oxide glassy electrolyte is mainly composed of network-modified oxides (Li_2O) and network oxides (such as SiO_2, P_2O_5, B_2O_3, etc.), and in general, the conductivity is about 10^{-6} S cm^{-1}. The concentration of Li$^+$ can be increased by increasing the content of Li_2O or adding some lithium salt, so as to improve the conductivity of the material. LiPON with the improved ionic conductivity can be formed by introducing nitrogen into Li_2O–P_2O_5 oxide glass solid electrolyte [92]; meanwhile, the thermal stability, the hardness of the glass, and the ability to resist the corrosion of water and salt solution have also been significantly improved. In addition, the introduction of ceramic crystal phase to form glass ceramic composite electrolyte can also improve the ionic conductivity of the material.

The ion conductivity of sulfide glassy electrolyte prepared by using S^{2-} with larger ion radius and higher polarity to replace O^{2-} in the oxide glass electrolyte system

can reach 10^{-3} S cm^{-1} [103]. The developing trend of solid-state sulfide electrolytes is shown in Figure 1.26. However, the environmental and equipment conditions during the preparation process are crucial due to the intrinsic sensitivity of the raw materials to air and water.

1.5 Separators

Battery separators are electric insulating membranes placed between cathodes and anodes. They have complex three-dimensional porous structures. When liquid electrolyte fills in, the separator allows rapid transfer of lithium ions between cathode and anode, which are necessary to complete the circuit of the battery. Moreover, separators are electrically insulating. Thus, the cathodes and anodes are physically isolated apart, which otherwise would lead to internal short-circuiting.

Although separators are not active components in batteries, it can be seen from the above discussion that the separator is very important for the lithium-ion battery system, and its structure and performance directly affect the performance of the whole battery [105]. Some key parameters influencing the battery safety are as follows.

- Thickness. The thickness controls the mechanical strength of the separators and the impedance of the lithium-ion battery. The thicker the separators, the better the mechanical strength, the stronger the piercing resistance. However, the increase of thickness will also increase the internal resistance of lithium-ion battery, reduce the utilization of active substances, and reduce the battery capacity. The thickness of separators is generally required to be less than 25 μm.
- Permeability. The permeability refers to the time required for gas to pass through the separators per unit area under a certain pressure, generally using Gurley value to evaluate. The smaller the Gurley value is, the shorter the time for gas to pass through the separators and the faster the gas speed is, the larger the pore and porosity are. The pressure drop method is generally used to determine the Gurley value of the separators. For commercial polyene separator, the Gurley value is generally less than 750 seconds. For a specific separator, the permeability of the separator is positively related to the internal resistance. It is suggested that the pore structure of the separator affects the transport of lithium ions, so a low Gurley value represents the high air permeability and low resistance.
- Pore size and distribution. The pore size of the separator is strictly required, which must be submicron. This is because the self-discharge of lithium-ion battery is serious when the pore size of the separator is too high, while the small pore size will affect the lithium ion transport.
- Porosity. The porosity of separator is crucial for lithium-ion battery, which directly affects the core of the battery (transport of lithium ion and storage of electrolyte). The separator with high porosity has better lithium ion permeability, and at the same time, it can also provide the storage site for the electrolyte of the battery.
- Mechanical strength. During the LIB battery fabrication process, separators are wound with the electrodes under tension. Thus, there are some basic

Figure 1.26 Developing trend of solid-state sulfide electrolytes. Source: Changhong Wang et al. [104] Reproduced with permission of Royal Society of Chemistry.

requirements for the mechanical strength of a separator: a reasonable tensile strength to sustain the stress during battery assembly (take the Celgard 2325 as an example, the machine direction Tensile Strength is as high as $1700\,kgf\,cm^{-2}$); a high puncture strength to avoid penetration of electrode material through the separator (empirically, the puncture strength should be at least $>300\,g\,mil^{-1}$), a good mix penetration strength to avoid loose electrode particles penetration and short cell, which requires $>100\,kgf\,mil^{-1}$ for separators in LIBs [106]. It should be noted that the selection of battery materials should be considered based on the circumstances where they will be practically used. The possibilities of harsh conditions such as battery crush and mechanical drop off should be given considerable attention.

- Thermal stability. Most of the battery separator membranes are polymeric materials, which will shrink and wrinkle apparently above a certain temperature. Thus, the thermal shrinkage at the early stage of battery thermal runaway process should be minimized, otherwise the cathode and anode of the battery will physically contact and eventually lead to thermal runaway. The requirement is generally <5% thermal shrinkage after 60 minutes at $90\,°C$ (in a vacuum) [107].

- Wettability. The separators should wet out quickly and completely in typical battery electrolytes. Incomplete and nonuniform wetting of the separator could result in heterogeneous lithium ion flux and thus the possible plating of lithium dendrites, which may short-circuit the battery.

- Ionic conductivity. The ionic conductivity of the separators refers to the ionic flow energy of the separators after being fully wetted by the electrolyte. The performance of lithium-ion battery mainly depends on the ionic conductivity of the electrolyte in the separator. The ionic conductivity of the common organic liquid electrolyte at room temperature is 10^{-4}–$10^{-3}\,S\,cm^{-1}$. The separator prevents the electrodes from contacting; however, the volume occupied by the separator will undoubtedly reduce the capacity of electrolyte between electrodes, resulting in the reduction of the effective conductivity of electrolyte and increase of the resistance.

- Chemical and electrochemical stability. The separator is soaked by electrolyte for a long time, and it needs to exist stably in the battery for a long time without shrinkage or swelling by solvent, etc. At the same time, it cannot be degraded by the strong oxidizing electrolyte, and it is strictly electrochemical inert. The material determines the stability of the separator (solvent resistance, strong oxidation resistance, electrical resistance, and chemical stability). The electrochemical stability of the separator can be measured by linear voltammetry.

It is difficult to simultaneously meet all the requirements. Most of the commercial LIB separators are polyolefin membranes, e.g. PE and/or PP. And some other separator materials with different chemical components are also emerging in the literatures. The scheme in Figure 1.27 describes the primary considerations for the separator modification in improving the battery safety.
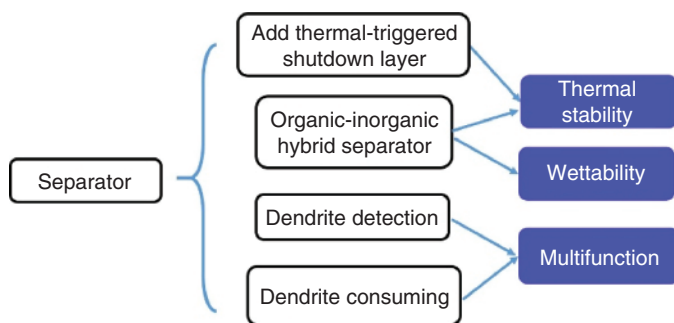
Figure 1.27 Scheme describing the primary considerations for the separator modification in improving the battery safety. Source: Yuan and Liu [108]. Reproduced with permission of Elsevier.

1.5.1 Polyolefin Separator

Due to its good insulation, low density, high mechanical strength, chemical resistance, and electrochemical corrosion resistance, almost all the separators for commercial lithium-ion batteries are made of semicrystalline polyolefin-based materials, such as PP, PE, and composite membranes of PP/PE/PP. The thickness of polyolefin separator used in 3 C electronic products is generally not greater than 25 μm. In order to meet the high power demand of HEV and EV, the thickness of separator is 32 and 40 μm, respectively. However, the polyolefin separators still have shortcomings. Firstly, due to the high crystallinity and low polarity of the polyolefin, the surface energy of the polyolefin separator is low, while the polarity of the electrolyte is high, and the affinity between the separator and the electrolyte is poor, so it is not easy to be infiltrated by the electrolyte, thus it makes the electrolyte easy to leak. Secondly, the porosity of polyolefin separator prepared by melt-drawing process is low, and the liquid absorption rate of the separator also decreases, which is not conducive to the migration of lithium ion and finally affects the electrochemical performance of the battery (rate performance and cycle stability). Thirdly, the thermal stability of polyolefin separator is limited, which may lead to temperature rise and even out of control of heat during overcharge, the separator began to shrink itself before shutting down the electrochemical reaction of the battery, resulting in the contact of positive and negative electrodes, causing short circuit and even explosion, thus posing a huge threat to the safety of lithium-ion battery. Among them, the major issue of polyolefin separators is their thermal instability. PP and PE are the most commonly used polyolefin separators, whereas their thermal stability is poor. The melting point (T_m) is just ~165 °C for PP and ~135 °C for PE [106], respectively. As temperatures approach their melting points, the separator shrinks dramatically in dimension. The internal short circuit of the battery happens and is further exaggerated afterward by the "positive feedback loop" (Figure 1.28), leading to thermal runaway. Several strategies have been employed to alleviate the safety issue of polyolefin-based separator.

A popular strategy is to employ multilayered structure to shut down the conduction pathway of lithium ions through the separator in case of overheating.

Separators with a PP/PE/PP trilayer structure have already been well commercialized (Figure 1.29a). When the internal temperature of the battery increases above ~130 °C, the porous middle PE layer partially melts, closing the pores inside the separator and preventing conduction of lithium ions in the liquid electrolytes (Figure 1.29b), while the PP layer provides mechanical support to maintain the overall dimensional stability, thus avoiding internal short-circuiting. The trilayer structure of the separator indeed has enhanced the safety of the LIBs. However, it does not always function well. In practical application, the heat in the cell could accumulate very quickly under harsh conditions and the internal temperature climbs up so fast that the thermal shutdown effect in PP/PE/PP can only last for a short duration due to the small melting temperature gap between PP and PE. Thus, the melting of the separator is still inevitable in some practical circumstances.
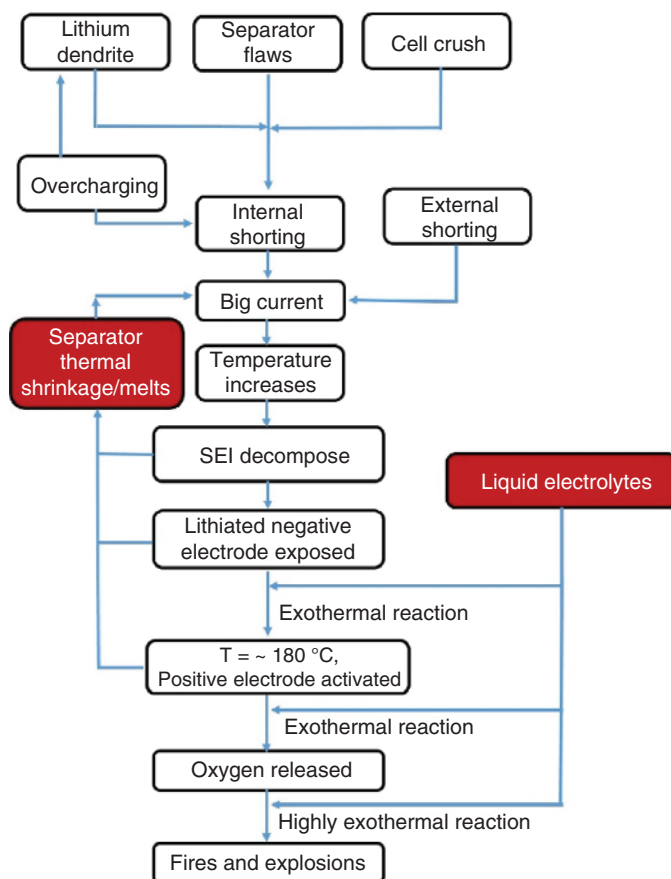

Figure 1.28 Flowchart illustrating the thermal runaway process. The key role of separator and liquid electrolyte is highlighted. Source: Yuan and Liu [108]. Reproduced with permission of Elsevier.
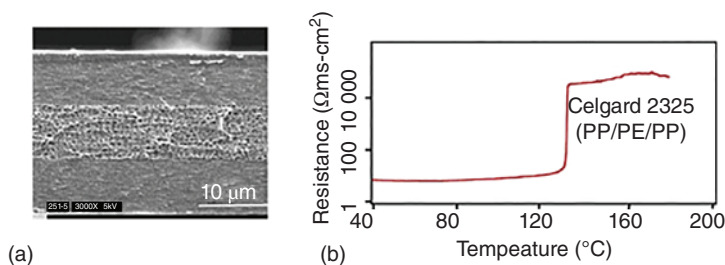
(a)   (b)

Figure 1.29 (a) Cross-section scanning electron micrographs of Celgard 2325 (PP/PE/PP) separator used in LIBs; (b) internal impedance (at 1 kHz) of Celgard 2325 (PP/PE/PP) separator as a function of temperature; heating rate: 60 °C min^{-1}. Source: Zhang et al. [106]. Reproduced with permission of American Chemical Society.

1.5.2 Polymers with High Melting Points for Separators

Porous membranes of poly(esters) [109], cellulose [110], polyimide [111], and other analogous have been demonstrated to be effective strategies to improve the thermal stability of separators (Figure 1.30a). For example, it has been reported that polyimide is a kind of thermosetting polymer widely considered as a promising alternative to polyolefin due to its excellent thermal stability (stable over 400 °C), high tensile strength, good electrolyte wettability, and flame retardancy, etc. (Figure 1.30b). The key step for preparing this kind of separator is to make inter-penetrated micro/nanopores as lithium ion transportation channel across these polymer membranes. In a recently reported work, recyclable LiBr was utilized as the template for nanopores creation. The fabrication was carried out at the intermediate polyamic acid stage of the polyimide, which shows much better processability. LiBr salt, used as the template, was mixed with the intermediates, and then the final mixture was casted into thin films after the chemical condensation reaction was finished. Uniform and interconnected nanopores across the thin membrane can be created by simply removing LiBr in the water bath. Once dissolved, LiBr can be further recycled. This facile synthesis method offers an exciting possibility for a PI separator both in lab-scale and potential manufacturing in industry.

1.5.3 Inorganic Composite Separators

The inorganic composite separator is based on a highly ordered porous structure matrix, which is coated with a layer of inorganic ceramic particles in the presence of high molecular organic adhesive. Due to its large specific surface area and good hydrophilicity, the inorganic ceramic particles exhibit excellent affinity with organic electrolyte solvents (ethylene carbonate [EC], propylene carbonate [PC], and buty-rolactone [GBL]); meanwhile, rigid inorganic particles can improve the thermal stability of the separator. The most common composition of ceramic coating is mainly composed of nonmetallic oxides such as SiO_2 and Al_2O_3 with hydroxyl groups on the surface, which are bonded with PVDF–HFP or PVDF. The characteristics of these nonmetallic oxides are that the particles are tightly stacked and the existing gap
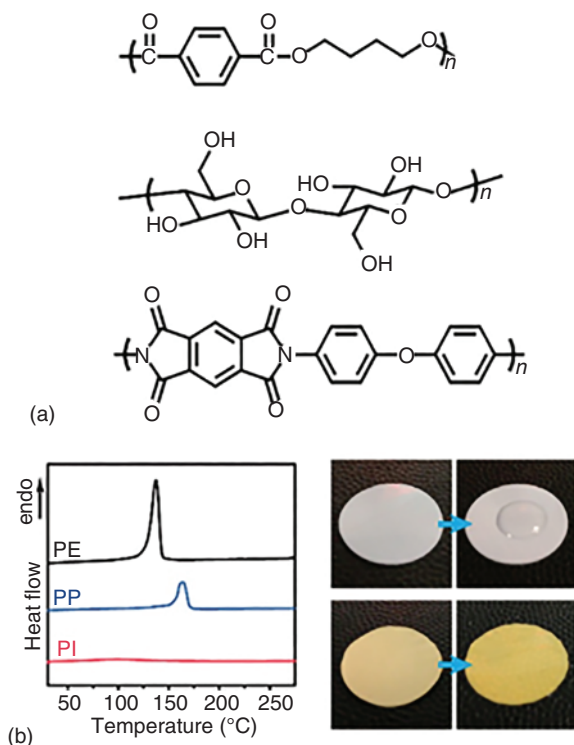
(a)

(b)

Figure 1.30 (a) Molecular structure of some high-melting temperature polymers as separator materials with low shrinkage at high temperatures. Top: polyimide (PI). Middle: cellulose. Bottom: poly(butylene) terephthalate. (b) Left: comparison of the differential scanning calorimetry (DSC) spectra of the PI with the PE and PP separator; the PI separator shows excellent thermal stability at the temperatures ranging from 30 to 275 °C. Right: digital camera photos comparing the wettability of a commercial separator and the as-synthesized PI separator with a propylene carbonate electrolyte. Source: Lin et al. [111]. Reproduced with permission of American Chemical Society.

provides a developed porous structure without affecting the air permeability and porosity of the separator, the thermal stability and liquid absorption of the separator can be improved. The most classical one is prepared by Kim et al. [112], who used PVDF–HFP as binder and coated SiO_2 particles on both sides of a commercial PE separator. It was found that the composite separators with SiO_2: PVDF–HFP of 9 : 1 possessed better porous structure, good liquid absorption, and high ionic conductivity and excellent thermal stability.

It should be noted that although numerous new materials have been reported in the literature, which are considered to be promising to replace the commercial polyolefin separators, few of them have been really commercialized. For practical applications, a good balance of the different parameters of the separators should be considered, such as mechanical strength, melting point, process ability, and cost.

1.6   Conclusions and Perspective

Energy density is the main issue of the batteries for commercial application. Lithium-ion batteries with high energy density are highly desired for the electric vehicles, portable devices, and large-scale energy storage techniques. Materials are crucial for the development of lithium-ion batteries, although various technologies have been developed to improve the electrochemical performance of the electrode materials, electrolytes, and separator, there are still many difficulties that limit their commercialization; thus, new materials design and full understanding of the charge/discharge mechanisms of the batteries are the two main challenges in the future. Incremental developments can be expected in the following four aspects:

Firstly, a thorough understanding of the deposition behavior of lithium as well as the formation mechanism and components of SEI film is the basis for the development of next-generation lithium-ion batteries. The advanced characterization methods such as freeze electron microscopy, environmental scanning electron microscopy, and in situ techniques need to be further developed to reveal the essence of the lithium-ion batteries.

Secondly, the commercialized graphite-based anode materials limit their wider application due to their relatively low theoretical capacity, easy to form lithium dendrite, and low lithium-ion intercalation potential. Therefore, it is highly desirable to explore the substitute anode materials with high electrochemical performance. Ideally, the optimized architecture, geometry, and compositions of materials will impart the electrode with high stability and high energy density simultaneously.

Thirdly, the low energy density is the main reason for the limited application of lithium-ion batteries at present, and the development lag of cathode materials is the bottleneck of the improvement of energy density of lithium-ion batteries. Lithium-rich manganese-based materials have high discharge capacity and wide voltage window, which are considered as the main candidates for the next generation of high-performance lithium-ion battery cathode materials. Therefore, how to solve the issues such as low first coulomb efficiency, poor cycling performance, continuous voltage attenuation, and so on, which hinder the practical application of materials, needs to be further researched.

Fourthly, the traditional lithium ion separator is difficult to adapt for the lithium-ion batteries with lithium metal as the anode and flexible lithium-ion batteries with bending. Therefore, further efforts should be made in the polymer electrolyte system with spectral suitability, such as the gel electrolyte based on the covalent self-cross-linking system and ionic liquid gel electrolytes based on the curved cross-linking system.

Last but not least, all solid-state lithium-ion batteries are thought to be the most promising candidate for the next-generation lithium-ion batteries with high energy density. Compared with organic electrolyte, solid electrolyte has lower ionic conductivity and better machining performance. Therefore, how to realize the thin-film electrolyte to promote the development of all solid-state thin-film battery will be an important research direction in the future.

Acknowledgments

References

1 Wang, J., Song, W.L., Wang, Z.Y. et al. (2015). Facile fabrication of binder-free metallic tin nanoparticle/carbon nanofiber hybrid electrodes for lithium-ion batteries. *Electrochim. Acta* 153: 468–475.

2 Ji, X.X., Huang, X.T., Liu, J.P. et al. (2010). Carbon-coated SnO(2) nanorod array for lithium-ion battery anode material. *Nanoscale Res. Lett.* 5: 649–653.

3 Xue, X.Y., Chen, Z.H., Xing, L.L. et al. (2011). SnO_2/alpha-MoO_3 core-shell nanobelts and their extraordinarily high reversible capacity as lithium-ion battery anodes. *Chem. Commun.* 47: 5205–5207.

4 Thomas, R. and Rao, G.M. (2015). SnO_2 nanowire anchored graphene nanosheet matrix for the superior performance of Li-ion thin film battery anode. *J. Mater. Chem. A* 3: 274–280.

5 Zhou, D., Song, W.L., and Fan, L.Z. (2015). Hollow core-shell SnO_2/C fibers as highly stable anodes for lithium-ion batteries. *Acs Appl. Mater. Inter.* 7: 21472–21478.

6 Mauger, A., Armand, M., Julien, C.M., and Zaghib, K. (2017). Challenges and issues facing lithium metal for solid-state rechargeable batteries. *J. Power Sources* 353: 333–342.

7 Patil, A., Choi, J.W., and Yoon, S.J. (2006). Review of issue and challenges facing rechargeable nanostructured lithium batteries. *IEEE Nmdc 2006: IEEE Nanotechnology Materials and Devices Conference 2006, Proceedings*, 196–197.

8 Patil, A., Patil, V., Shin, D.W. et al. (2008). Issue and challenges facing rechargeable thin film lithium batteries. *Mater. Res. Bull.* 43: 1913–1942.

9 Tarascon, J.M. and Armand, M. (2001). Issues and challenges facing rechargeable lithium batteries. *Nature* 414: 359–367.

10 Zhou, L.M., Zhang, K., Hu, Z. et al. (2018). Recent developments on and prospects for electrode materials with hierarchical structures for lithium-ion batteries. *Adv. Energy Mater.* 8: 1701415.

11 Wang, Y., Niu, S.S., and Lu, S. (2015). Controlled-synthesis and lithium storage properties of SnO_2 porous core-shell spheres and core-in-double-shell spheres. *Mater. Lett.* 157: 209–211.

12 Erickson, E.M., Schipper, F., Penki, T.R. et al. (2017). Review-recent advances and remaining challenges for lithium ion battery cathodes: II. Lithium-rich, xLi subset of 2 subset of MnO subset of 3 subset of (1-x)LiNi subset of a subset

of co subset of b subset of Mn subset of c subset of O subset of 2 subset of. *J. Electrochem. Soc.* 164: A6341–A6348.

13 Manthiram, A., Song, B., and Li, W. (2017). A perspective on nickel-rich layered oxide cathodes for lithium-ion batteries. *Energy Storage Materials* 6: 125–139.

14 Wang, G.X., Zhong, S., Bradhurst, D.H. et al. (1998). Synthesis and characterization of LiNiO compounds as cathodes for rechargeable lithium batteries. *J. Power Sources* 76: 141–146.

15 Cho, J.P., Kim, T.J., and Park, B. (2002). The effect of a metal-oxide coating on the cycling behavior at 55 degrees C in orthorhombic $LiMnO_2$ cathode materials. *J. Electrochem. Soc.* 149: A288–A292.

16 Liu, Z.L., Yu, A.S., and Lee, J.Y. (1999). Synthesis and characterization of $LiNi_{1-x-y}Co_xMn_yO_2$ as the cathode materials of secondary lithium batteries. *J. Power Sources* 81: 416–419.

17 Ryu, H.-H., Park, K.-J., Yoon, C.S., and Sun, Y.-K. (2018). Capacity fading of Ni-rich $Li[Ni_xCo_yMn_{1-x-y}]O_2$ ($0.6 \leq x \leq 0.95$) cathodes for high-energy-density lithium-ion batteries: bulk or surface degradation? *Chem. Mater.* 30: 1155–1163.

18 Mukherjee, P., Faenza, N.V., Pereira, N. et al. (2018). Surface structural and chemical evolution of layered $LiNi_{0.8}Co_{0.15}Al_{0.050}O_2$ (NCA) under high voltage and elevated temperature conditions. *Chem. Mater.* 30: 8431–8445.

19 Xia, H., Xia, Q.Y., Lin, B.H. et al. (2016). Self-standing porous $LiMn_2O_4$ nanowall arrays as promising cathodes for advanced 3D microbatteries and flexible lithium-ion batteries. *Nano Energy* 22: 475–482.

20 Lee, M.J., Lee, S., Oh, P. et al. (2014). High performance $LiMn_2O_4$ cathode materials grown with epitaxial layered nanostructure for Li-ion batteries. *Nano Lett.* 14: 993–999.

21 Chen, R.J., Zhao, T.L., Zhang, X.X. et al. (2016). Advanced cathode materials for lithium-ion batteries using nanoarchitectonics. *Nanoscale Horiz.* 1: 423–444.

22 Nakayama, M., Yamada, S., Jalem, R., and Kasuga, T. (2016). Density functional studies of olivine-type $LiFePO_4$ and $NaFePO_4$ as positive electrode materials for rechargeable lithium and sodium ion batteries. *Solid State Ionics* 286: 40–44.

23 Cheng, H., Shapter, J.G., Li, Y., and Gao, G. (2021). Recent progress of advanced anode materials of lithium-ion batteries. *J. Energy Chem.* 57: 451–468.

24 Nitta, N., Wu, F.X., Lee, J.T., and Yushin, G. (2015). Li-ion battery materials: present and future. *Mater. Today* 18: 252–264.

25 Tian, Q.H., Chen, P., Zhang, Z.X., and Yang, L. (2017). Achievement of significantly improved lithium storage for novel clew-like $Li_4Ti_5O_{12}$ anode assembled by ultrafine nanowires. *J. Power Sources* 350: 49–55.

26 Zhang, Y.X., Luo, Y., Chen, Y. et al. (2017). Enhanced rate capability and low-temperature performance of $Li_4Ti_5O_{12}$ anode material by facile surface fluorination. *ACS Appl. Mater. Inter.* 9: 17146–17155.

27 Nishi, Y. (2001). The development of lithium ion secondary batteries. *Chem. Rec.* 1: 406–413.

28 Endo, M., Kim, C., Nishimura, K. et al. (2000). Recent development of carbon materials for Li ion batteries. *Carbon* 38: 183–197.

29 Liu, D.Q., Liu, Z.J., Li, X.W. et al. (2017). Group IVA element (Si, Ge, Sn)-based alloying/dealloying anodes as negative electrodes for full-cell lithium-ion batteries. *Small* 13: 1702000.

30 Guo, J.X., Zhu, H.F., Sun, Y.F. et al. (2017). Pie-like free-standing paper of graphene paper@Fe_3O_4 nanorod array@carbon as integrated anode for robust lithium storage. *Chem. Eng. J.* 309: 272–277.

31 Yu, S.H., Lee, S.H., Lee, D.J. et al. (2016). Conversion reaction-based oxide nanomaterials for lithium ion battery anodes. *Small* 12: 2146–2172.

32 Lou, X.W., Li, C.M., and Archer, L.A. (2009). Designed synthesis of coaxial SnO_2@carbon hollow nanospheres for highly reversible lithium storage. *Adv. Mater.* 21: 2536.

33 Wang, C., Zhou, Y., Ge, M.Y. et al. (2010). Large-scale synthesis of SnO_2 nanosheets with high lithium storage capacity. *J. Am. Chem. Soc.* 132: 46–47.

34 Jin, Y.H., Min, K.M., Seo, S.D. et al. (2011). Enhanced Li storage capacity in 3 nm diameter SnO_2 nanocrystals firmly anchored on multiwalled carbon nanotubes. *J. Phys. Chem. C* 115: 22062–22067.

35 Liang, J., Yu, X.Y., Zhou, H. et al. (2014). Bowl-like SnO_2@carbon hollow particles as an advanced anode material for lithium-ion batteries. *Angew. Chem. Int. Ed.* 53: 12803–12807.

36 Ren, J.G., Yang, J.B., Abouimrane, A. et al. (2011). SnO_2 nanocrystals deposited on multiwalled carbon nanotubes with superior stability as anode material for Li-ion batteries. *J. Power Sources* 196: 8701–8705.

37 Hu, R.Z., Chen, D.C., Waller, G. et al. (2016). Dramatically enhanced reversibility of Li_2O in SnO_2-based electrodes: the effect of nanostructure on high initial reversible capacity. *Energy Environ. Sci.* 9: 595–603.

38 Zhou, X.S., Wan, L.J., and Guo, Y.G. (2013). Binding SnO_2 nanocrystals in nitrogen-doped graphene sheets as anode materials for lithium-ion batteries. *Adv. Mater.* 25: 2152–2157.

39 Zhao, S., Sewell, C.D., Liu, R. et al. (2019). SnO_2 as advanced anode of alkali-ion batteries: inhibiting Sn coarsening by crafting robust physical barriers, void boundaries, and heterophase interfaces for superior electrochemical reaction reversibility. *Adv. Energy Mater.*: 1902657.

40 Lang, J., Long, Y., Qu, J. et al. (2019). One-pot solution coating of high quality LiF layer to stabilize Li metal anode. *Energy Storage Mater.* 16: 85–90.

41 Adair, K.R., Iqbal, M., Wang, C. et al. (2018). Towards high performance Li metal batteries: nanoscale surface modification of 3D metal hosts for pre-stored Li metal anodes. *Nano Energy* 54: 375–382.

42 Wang, Q., Yang, C., Yang, J. et al. (2018). Stable Li metal anode with protected interface for high-performance Li metal batteries. *Energy Storage Mater.* 15: 249–256.

43 Yun, Q.B., He, Y.B., Lv, W. et al. (2016). Chemical dealloying derived 3D porous current collector for Li metal anodes. *Adv. Mater.* 28: 6932.

44 Xu, W., Wang, J.L., Ding, F. et al. (2014). Lithium metal anodes for rechargeable batteries. *Energy Environ. Sci.* 7: 513–537.

45 Cheng, X.B., Zhang, R., Zhao, C.Z., and Zhang, Q. (2017). Toward safe lithium metal anode in rechargeable batteries: a review. *Chem. Rev.* 117: 10403–10473.

46 Huang, K., Li, Z., Xu, Q. et al. (2019). Lithiophilic CuO nanoflowers on Ti-mesh inducing lithium lateral plating enabling stable lithium-metal anodes with ultrahigh rates and ultralong cycle life. *Adv. Energy Mater.* 9.

47 Li, T., Shi, P., Zhang, R. et al. (2019). Dendrite-free sandwiched ultrathin lithium metal anode with even lithium plating and stripping behavior. *Nano Res.* 12: 2224–2229.

48 Jiao, S., Zheng, J., Li, Q. et al. (2018). Behavior of lithium metal anodes under various capacity utilization and high current density in lithium metal batteries. *Joule* 2: 110–124.

49 Zou, P., Wang, Y., Chiang, S.W. et al. (2018). Directing lateral growth of lithium dendrites in micro-compartmented anode arrays for safe lithium metal batteries. *Nat. Commun.* 9: 464.

50 Goodenough, J.B. and Kim, Y. (2010). Challenges for rechargeable Li batteries. *Chem. Mater.* 22: 587–603.

51 Goodenough, J.B. and Park, K.S. (2013). The Li-ion rechargeable battery: a perspective. *J. Am. Chem. Soc.* 135: 1167–1176.

52 Dong, H.Y., Xiao, X.L., Jin, C. et al. (2019). High lithium-ion conductivity polymer film to suppress dendrites in Li metal batteries. *J. Power Sources* 423: 72–79.

53 Cheng, X.B., Yan, C., Chen, X. et al. (2017). Implantable solid electrolyte inter-phase in lithium-metal batteries. *Chem-Us* 2: 258–270.

54 Tao, R., Bi, X.X., Li, S. et al. (2017). Kinetics tuning the electrochemistry of lithium dendrites formation in lithium batteries through electrolytes. *ACS Appl. Mater. Inter.* 9: 7003–7008.

55 Li, X., Zheng, J., Ren, X. et al. (2018). Dendrite-free and performance-enhanced lithium metal batteries through optimizing solvent compositions and adding combinational additives. *Adv. Energy Mater.* 8.

56 Zhang, X.-Q., Cheng, X.-B., Chen, X. et al. (2017). Fluoroethylene carbonate additives to render uniform Li deposits in lithium metal batteries. *Adv. Funct. Mater.* 27.

57 Wan, H., Peng, G., Yao, X. et al. (2016). Cu_2ZnSnS_4/graphene nanocomposites for ultrafast, long life all-solid-state lithium batteries using lithium metal anode. *Energy Storage Mater.* 4: 59–65.

58 Bouchet, R., Maria, S., Meziane, R. et al. (2013). Single-ion BAB triblock copolymers as highly efficient electrolytes for lithium-metal batteries. *Nat. Mater.* 12: 452–457.

59 Liu, R., Wu, Z., He, P. et al. (2019). A self-standing, UV-cured semi-interpenetrating polymer network reinforced composite gel electrolytes for dendrite-suppressing lithium ion batteries. *J. Materiomics* 5: 185–194.

60 A. Varzi, L. Mattarozzi, S. Cattarin, P. Guerriero, S. Passerini, (2018). *3D porous Cu-Zn alloys as alternative anode materials for Li-ion batteries with superior low T performance. Adv. Energy Mater.*, 8. https://doi.org/10.1002/aenm.201701706

61 Peng, Z., Ren, F.H., Yang, S.S. et al. (2019). A highly stable host for lithium metal anode enabled by Li_9Al_4-Li_3N-AlN structure. *Nano Energy* 59: 110–119.

62 Guo, F., Wang, Y., Kang, T. et al. (2018). A Li-dual carbon composite as stable anode material for Li batteries. *Energy Storage Mater.* 15: 116–123.

63 Liu, B., Zhang, L., Xu, S. et al. (2018). 3D lithium metal anodes hosted in asymmetric garnet frameworks toward high energy density batteries. *Energy Storage Mater.* 14: 376–382.

64 Yue, X.-Y., Wang, W.-W., Wang, Q.-C. et al. (2018). CoO nanofiber decorated nickel foams as lithium dendrite suppressing host skeletons for high energy lithium metal batteries. *Energy Storage Mater.* 14: 335–344.

65 Wang, L., Zhu, X., Guan, Y. et al. (2018). ZnO/carbon framework derived from metal-organic frameworks as a stable host for lithium metal anodes. *Energy Storage Mater.* 11: 191–196.

66 Zhao, Q., Liu, X., Stalin, S. et al. (2019). Solid-state polymer electrolytes with in-built fast interfacial transport for secondary lithium batteries. *Nat. Energy* 4: 365–373.

67 Aravindan, V., Gnanaraj, J., Madhavi, S., and Liu, H.K. (2011). Lithium-ion conducting electrolyte salts for lithium batteries. *Chem.-Eur. J.* 17: 14326–14346.

68 Kita, F., Sakata, H., Sinomoto, S. et al. (2000). Characteristics of the electrolyte with fluoro organic lithium salts. *J. Power Sources* 90: 27–32.

69 Edman, L., Doeff, M.M., Ferry, A. et al. (2000). Transport properties of the solid polymer electrolyte system P(EO)(n)LiTFSI. *J. Phys. Chem. B* 104: 3476–3480.

70 Campion, C.L., Li, W.T., and Lucht, B.L. (2005). Thermal decomposition of $LiPF_6$-based electrolytes for lithium-ion batteries. *J. Electrochem. Soc.* 152: A2327–A2334.

71 Zhang, S.S., Xu, K., and Jow, T.R. (2002). Study of $LiBF_4$ as an electrolyte salt for a Li-ion battery. *J. Electrochem. Soc.* 149: A586–A590.

72 Ding, M.S. and Jow, T.R. (2004). How conductivities and viscosities of PC-DEC and PC-EC solutions of $LiBF_4$, $LiPF_6$, LiBOB, Et_4NBF_4, and Et_4NPF_6 differ and why. *J. Electrochem. Soc.* 151: A2007–A2015.

73 Zhou, H.M., Liu, F.R., and Li, J. (2012). Preparation, thermal stability and electrochemical properties of LiODFB. *J. Mater. Sci. Technol.* 28: 723–727.

74 Zhang, S.S., Xu, K., and Jow, T.R. (2006). Study of the charging process of a LiCoO(2)-based Li-ion battery. *J. Power Sources* 160: 1349–1354.

75 Zhang, S.S., Xu, K., and Jow, T.R. (2002). A new approach toward improved low temperature performance of Li-ion battery. *Electrochem. Commun.* 4: 928–932.

76 Herreyre, S., Huchet, O., Barusseau, S. et al. (2001). New Li-ion electrolytes for low temperature applications. *J. Power Sources* 97-8: 576–580.

77 Liao, L.X., Cheng, X.Q., Ma, Y.L. et al. (2013). Fluoroethylene carbonate as electrolyte additive to improve low temperature performance of $LiFePO_4$ electrode. *Electrochim. Acta* 87: 466–472.

78 Zhang, S.S. (2006). An unique lithium salt for the improved electrolyte of Li-ion battery. *Electrochem. Commun.* 8: 1423–1428.

79 Chung, G.C., Kim, H.J., Yu, S.I. et al. (2000). Origin of graphite exfoliation – an investigation of the important role of solvent cointercalation. *J. Electrochem. Soc.* 147: 4391–4398.

80 Lee, D.J., Im, D., Ryu, Y.G. et al. (2013). Phosphorus derivatives as electrolyte additives for lithium-ion battery: the removal of O-2 generated from lithium-rich layered oxide cathode. *J. Power Sources* 243: 831–835.

81 Bachman, J.C., Muy, S., and Grimaud, A. (2016). Inorganic solid-state electrolytes for lithium batteries: mechanisms and properties governing ion conduction. *Chem. Rev.* 116: 140–162.

82 Takada, K. (2013). Progress and prospective of solid-state lithium batteries. *Acta Mater.* 61: 759–770.

83 Stoeva, Z., Martin-Litas, I., Staunton, E. et al. (2003). Ionic conductivity in the crystalline polymer electrolytes PEO_6: $LiXF_6$, X = P, As, Sb. *J. Am. Chem. Soc.* 125: 4619–4626.

84 Shin, J.H., Henderson, W.A., Scaccia, S. et al. (2006). Solid-state $Li/LiFePO_4$ polymer electrolyte batteries incorporating an ionic liquid cycled at 40 degrees C. *J. Power Sources* 156: 560–566.

85 Nakano, H., Dokko, K., Sugaya, J.I. et al. (2007). All-solid-state micro lithium-ion batteries fabricated by using dry polymer electrolyte with micro-phase separation structure. *Electrochem. Commun.* 9: 2013–2017.

86 Stephan, A.M. (2006). Review on gel polymer electrolytes for lithium batteries. *Eur. Polym. J.* 42: 21–42.

87 Gregory, D.H., O'Meara, P.M., Gordon, A.G. et al. (2002). Structure of lithium nitride and transition-metal-doped derivatives, $Li_{3-x-y}MxN$ (M = Ni, Cu): a powder neutron diffraction study. *Chem. Mater.* 14: 2063–2070.

88 Varez, A., Fernández-Díaz, M.T., Alonso, J.A., and Sanz, J. (2005). Structure of fast ion conductors $Li_3xLa_{2/3-x}TiO_3$ deduced from powder neutron diffraction experiments. *Chem. Mater.* 17: 2404–2412.

89 Morata-Orrantia, A., Garcia-Martin, S., and Alario-Franco, M.A. (2003). Optimization of lithium conductivity in La/Li titanates. *Chem. Mater.* 15: 3991–3995.

90 Deng, Y., Eames, C., Fleutot, B. et al. (2017). Enhancing the lithium ion conductivity in lithium superionic conductor (LISICON) solid electrolytes through a mixed polyanion effect. *ACS Appl. Mater. Interfaces* 9: 7050–7058.

91 Knauth, P. (2009). Inorganic solid Li ion conductors: an overview. *Solid State Ionics* 180: 911–916.

92 Song, S.W., Choi, H., Park, H.Y. et al. (2010). High rate-induced structural changes in thin-film lithium batteries on flexible substrate. *J. Power Sources* 195: 8275–8279.

93 Hassoun, J., Verrelli, R., Reale, P. et al. (2013). A structural, spectroscopic and electrochemical study of a lithium ion conducting $Li_{10}GeP_2S_{12}$ solid electrolyte. *J. Power Sources* 229: 117–122.

94 Ong, S.P., Mo, Y.F., Richards, W.D. et al. (2013). Phase stability, electrochemical stability and ionic conductivity of the Li10 +/− 1MP2X12 (M = Ge, Si, Sn, Al or P, and X = O, S or Se) family of superionic conductors. *Energy Environ. Sci.* 6: 148–156.

95 Anantharamulu, N., Rao, K.K., Rambabu, G. et al. (2011). A wide-ranging review on Nasicon type materials. *J. Mater. Sci.* 46: 2821–2837.

96 Jackman, S.D. and Cutler, R.A. (2013). Stability of NaSICON-type $Li_{1.3}Al_{0.3}Ti_{1.7}P_3O_{12}$ in aqueous solutions. *J. Power Sources* 230: 251–260.

97 Swamy, D.T., Babu, K.E., and Veeraiah, V. (2013). Evidence for high ionic conductivity in lithium-lanthanum titanate, Li0 center dot 29La0 center dot 57TiO$_3$. *B Mater. Sci.* 36: 1115–1119.

98 Thangadurai, V., Adams, S., and Weppner, W. (2004). Crystal structure revision and identification of Li^+-ion migration pathways in the garnet-like $Li_5La_3M_2O_{12}$ (M = Nb, Ta) oxides. *Chem. Mater.* 16: 2998–3006.

99 Thangadurai, V. and Weppner, W. (2005). Li(6)ALa(2)Ta(2)O(12) (A=Sr, Ba): Novel garnet-like oxides for fast lithium ion conduction. *Adv. Funct. Mater.* 15: 107–112.

100 Thangadurai, V., Kaack, H., and Weppner, W.J.F. (2003). Novel fast lithium ion conduction in garnet-type $Li_5La_3M_2O_{12}$ (M = Nb, Ta). *J. Am. Ceram. Soc.* 86: 437–440.

101 Narayanan, S., Baral, A.K., and Thangadurai, V. (2016). Dielectric characteristics of fast Li ion conducting garnet-type $Li_{5+2x}La_3Nb_{2-x}YxO_{12}$ (x = 0.25, 0.5 and 0.75). *Phys. Chem. Chem. Phys.* 18: 15418–15426.

102 Ahmad, M.M. and Al-Jaafari, A. (2015). Concentration and mobility of mobile Li^+ ions in $Li_6BaLa_2Ta_2O_{12}$ and $Li_5La_3Ta_2O_{12}$ garnet lithium ion conductors. *J. Mater. Sci.-Mater. El* 26: 8136–8142.

103 Ohtomo, T., Hayashi, A., Tatsumisago, M. et al. (2013). All-solid-state lithium secondary batteries using the 75Li(2)S center dot 25P(2)S(5) glass and the 70Li(2)S center dot 30P(2)S(5) glass-ceramic as solid electrolytes. *J. Power Sources* 233: 231–235.

104 Wang, C., Liang, J., Zhao, Y. et al. (2009). All-solid-state lithium batteries enabled by sulfide electrolytes: from fundamental research to practical engineering design. *Energy Environ. Sci.* 14: 2577–2619.

105 Lee, H., Yanilmaz, M., Toprakci, O. et al. (2014). A review of recent developments in membrane separators for rechargeable lithium-ion batteries. *Energy Environ. Sci.* 7: 3857–3886.

106 Zhang, P.A.Z.J. (2004). Battery separators. *Chem. Rev.* 104: 4419–4462.

107 Zhang, S.S. (2007). A review on the separators of liquid electrolyte Li-ion batteries. *J. Power Sources* 164: 351–364.

108 Yuan, M.Q. and Liu, K. (2020). Rational design on separators and liquid electrolytes for safer lithium-ion batteries. *J. Energy Chem.* 43: 58–70.

109 Orendorff, C.J., Lambert, T.N., Chavez, C.A. et al. (2013). Polyester separators for lithium-ion cells: improving thermal stability and abuse tolerance. *Adv. Energy Mater.* 3: 314–320.

110 Li, L., Yu, M., Jia, C. et al. (2017). Cellulosic biomass-reinforced polyvinylidene fluoride separators with enhanced dielectric properties and thermal tolerance. *ACS Appl. Mater. Inter.* 9: 20885–20894.

111 Lin, D.C., Zhuo, D., Liu, Y.Y., and Cui, Y. (2016). All-integrated bifunctional separator for Li dendrite detection via novel solution synthesis of a thermostable polyimide separator. *J. Am. Chem. Soc.* 138: 11044–11050.

112 Kim, K.J., Kim, J.H., Park, M.S. et al. (2012). Enhancement of electrochemical and thermal properties of polyethylene separators coated with polyvinylidene fluoride-hexafluoropropylene co-polymer for Li-ion batteries. *J. Power Sources* 198: 298–302.